DESIGN CONSIDERATIONS OF SOUTH AFRICAN RESIDENTIAL DISTRIBUTION SYSTEMS CONTAINING EMBEDDED GENERATION

by

Gustav Reinhold Krüger

Submitted in partial fulfilment of the requirements for the degree
Master of Engineering (Electrical Engineering)

in the

Department of Electrical, Electronic and Computer Engineering
Faculty of Engineering, Built Environment and Information Technology

UNIVERSITY OF PRETORIA

AUGUST 2017

SUMMARY

DESIGN CONSIDERATIONS OF SOUTH AFRICAN RESIDENTIAL DISTRIBUTION SYSTEMS CONTAINING EMBEDDED GENERATION

by

Gustav Reinhold Krüger

Supervisor: Dr R.M. Naidoo

Department: Electrical, Electronic and Computer Engineering

University: University of Pretoria

Degree: Master of Engineering (Electrical Engineering)

Keywords: Embedded Generation, Distributed Generation, High Density residential clusters, Distribution grid, Photo Voltaic System, H-Bridge inverter, Maximum Power Point Tracking

The electricity generation composition in the South African national grid has changed in recent years from mostly thermal generation to a combination of thermal generation plants and a variety of plants owned and operated by Renewable Energy Independent Power Producers (REIPPs). The need arises to determine whether the existing planning and design guidelines of distribution networks in South Africa are sufficient in terms of equipment specifications and general sizing and rating principles, used during the network planning process, under increasing penetration levels of embedded generation.

The correlation between increases in embedded generation penetration levels and voltage variation, unbalance and harmonic emissions are determined by simulating various operating scenarios of varying load and short circuit level for penetration levels of 10%, 25% and 40%. The existing distribution grid planning standard NRS 097 allows for a 25% penetration level where several consumers share one feeder or distribution transformer. Some of the limits contained in the South African power quality standards NRS 048 and the distribution grid planning guidelines NRS 097 are exceeded when penetration levels of grid connected Photovoltaic (PV) generation exceeds certain levels.

- Switching embedded generation in or out of service does not cause voltage variations that exceed the planning limit of 3% at the shared feeder.
- Voltage unbalance due to embedded generation connected to the same phase does not cause the compatibility limit of 3% to be exceeded.
- Current unbalance should be monitored as it is very likely that equipment ratings may be exceeded when the integration of embedded generation is not coordinated.
- Voltage harmonic limits of the odd harmonic which are multiples of 3 are exceeded.
- Current harmonic planning limits of several harmonics are exceeded for penetration levels of 25%.

The criteria and limits contained in the standards and guidelines relating to current unbalance and harmonic currents should be reviewed to ensure that future grids with high penetration levels of embedded generation can withstand the inherent power quality challenges without having an adverse effect on distribution equipment. Distribution transformers can age faster when they are subjected to harmonic currents and voltages exceeding their design parameters [12]. The distribution transformer isolates the Medium Voltage (MV) distribution grid from the 400 V residential grid. The voltage harmonics and voltage unbalance on the Low Voltage (LV) grid therefore do not permeate to the MV grid. Proposed future work includes translating the qualitative suggestions made in this dissertation into quantitative terms that can be included in revisions of the distribution equipment standards and grid planning guidelines.

LIST OF ABBREVIATIONS

AC	Alternating Current
CFL	Compact Fluorescent Light
DC	Direct Current
EG	Embedded Generation
HV	High Voltage
LV	Low Voltage
MPPT	Maximum Power Point Tracker
MV	Medium Voltage
NERSA	National Energy Regulator of South Africa
NMD	Notified Maximum Demand
OLTC	On-Load Tap Changers
PCC	Point of Common Coupling
pdf	probability density function
POC	Point Of Connection
PV	Photo Voltaic
REIPP	Renewable Energy Independent Power Producer
RMS	Root Mean Squared
RSS	Root Sum Squared
THD	Total Harmonic Distortion

TABLE OF CONTENTS

LIST OF FIGURES

LIST OF TABLES

CHAPTER 1 INTRODUCTION

1.1 PROBLEM STATEMENT

The electricity generation composition in the South African national grid has changed in recent years from mostly thermal generation to a combination of thermal generation plants and a variety of plants owned and operated by Renewable Energy Independent Power Producers (REIPPs). In 2011, the South African Department of Energy introduced the procurement program for REIPPs in a bid to integrate 3725 MW into the national grid by 2030. This plan mirrors international efforts and plans to reduce global carbon emissions. The global move towards renewable energy sources has reduced the cost of the various renewable energy technologies. It is now financially viable for individuals to generate their own power instead of purchasing electrical energy from a utility.

As yet, the South African utility Eskom and the municipalities and metros are responsible for the expansion, operation and maintenance of the distribution networks, regardless of the integration of independently operated small scale generation. The impact of integrating small scale embedded generation on the existing distribution grid and electrical equipment requires continuous assessment as the penetration levels of the distributed generation increase. The national energy regulator (NERSA) has the obligation to assess generation and distribution license applications from individuals as well as private and public entities and evaluate the impact of the proposed energy projects on existing infrastructure, the environment and on society before issuing a generation or distribution license. The impact on the electrical grid of any connection is project dependent and technical of nature and it is challenging to estimate the outcome without performing grid integration studies. The Grid Connection Code for REIPPs contains very lax requirements for generation plants smaller than 13.8 kVA, classified as type A1. The grid connection code requirements for small rooftop Photovoltaic (PV) systems in terms of power quality aspects are often not

implemented for such small plants as the assessment process and associated cost does not justify the impact of any individual installation.

This lack in oversight over small scale PV system integration may lead to challenges that need to be addressed in the distribution system planning and design cycle. The effect of small scale PV embedded generation on power quality and thereby on the distribution grid equipment and planning criteria has to be investigated before any mitigating measures can be taken. It must be determined whether the existing planning and design guidelines of distribution networks in South Africa are sufficient in terms of equipment specifications and general sizing and rating principles, used during the network planning process, under increasing penetration levels of embedded generation.

1.2 RESEARCH GAP

The principles and methods used to size and rate distribution equipment are being refined and reviewed on a continuous basis as urban and suburban growth patterns evolve. The standards that guide the practical implementation usually lag the research as shortcomings of existing standards manifest themselves in equipment failures before action is taken. Power quality challenges are historically only prevalent in high voltage transmission systems where industrial loads and commercial power generation are integrated. The IEEE Standard 1159 defines power quality as "the concept of powering and grounding sensitive equipment in a manner that is suitable to the operation of that equipment". With the advent of high penetration levels of embedded PV generation in residential areas, some of the power quality challenges prevalent on transmission level networks are expected to affect distribution grids. Historically, the urban distribution network only served to feed domestic loads that were mostly passive constant impedance loads with near ideal power factor. Research in the field of power quality challenges in distribution grids is gaining a strong foothold. The research gap addressed in this dissertation pertains to the design and planning guidelines of distribution grids and whether these have evolved sufficiently to take an evolving load profile in conjunction with embedded generation into consideration to prevent equipment failures and to ensure that the expected equipment life cycles are met. The research in this dissertation is applicable to high density residential clusters with high penetration levels of PV rooftop system embedded generation. The load profile and

distribution grid topology is based on a simulation model compiled according to South African planning guidelines and measurement results. The evaluation criteria are the planning and compatibility levels of South African power quality standards and the distribution equipment immunity levels.

1.3 RESEARCH OBJECTIVE AND QUESTIONS

The objective of this research is to evaluate the impact of embedded generation on existing distribution networks using a simulation tool developed specifically for this research. The tool is used to assess whether the existing planning and design guidelines of distribution networks in South Africa are sufficient in terms of specifications and general sizing and rating criteria used for distribution network planning.

The following research questions have to be answered in order to achieve this goal:

- Does the maximum permitted penetration level of embedded generation, according to planning guideline NRS 097, prevent power quality limits from being exceeded?
- How is the distribution grid equipment affected by various power quality aspects?
- Are further design standards required or can the challenges be mitigated by amending grid planning and equipment rating guidelines?

The questions are translated into the following objectives that have to be met in order to attain the research goal:

Objective 1: Define the power quality standards in quantitative terms

The literature review is instrumental to the objective of identifying the equipment and power quality standards and interpreting the constraints under which the various limits are applicable and how power quality is measured and assessed.

Objective 2: Identify study cases

It is not possible to study every possible scenario as the number of variables in the simulation models is extensive. It is therefore necessary to identify the most onerous cases and to assess the applicability of the outcome to other scenarios. A trial and error method is proposed to identify threshold cases considering the parameters of the planning guidelines.

Objective 3: Assess the effect of exceeding power quality limits

The objective is realised by reviewing existing research on failure mechanisms and evaluating how the life cycle of distribution equipment is affected by the power quality

aspects defined in Objective 1. This objective is met by qualitative analysis of the simulation results. International practices are referenced where available to propose improvements to the South African design standards and guidelines.

1.4 HYPOTHESIS AND APPROACH

A preliminary answer to the research questions is the following hypothesis:

The integration of embedded generation in high density residential housing distribution systems requires specific technical design and planning criteria in addition to those addressed in the planning guideline for distribution grids with integrated low-voltage, small-scale embedded generation.

A mixed-method research methodology is employed consisting of quantitative and empirical elements. An engineering-oriented approach is used to combine various established methods in a comprehensive simulation tool which is employed to evaluate quantitative criteria. The hypothesis is quantified by the numerical criteria contained in existing standards and guidelines and tested within a subjectively defined framework, based on empirical data, to arrive at the conclusion which is qualitative of nature.

1.5 RESEARCH GOALS

The first goal of this research is to identify and quantify power quality criteria used in distribution grid planning guidelines pertaining to equipment sizing and rating. The criteria are based on the NRS 048 power quality planning and compliance standards, interpreted objectively in accordance with the NRS 097:2014 guidelines to address power quality challenges in high density residential cluster distribution grids.

A further goal of the research is to assess and qualify the effects of adverse power quality, due to high penetration levels of small rooftop PV systems in high density residential clusters, on distribution equipment life cycles. The outcomes of the research must highlight possible shortcomings of existing standards and methods of assessment that might be encountered in future grids with high penetration levels of small rooftop PV systems. The methods employed in attaining these goals are based on established research and simulation study methods to promote research continuity and introduce further research ideas.

1.6 RESEARCH CONTRIBUTION

The research presented in this dissertation focusses on the integration of embedded generation in distribution networks of high density residential complexes. South African low voltage distribution network planning standards and guidelines are evaluated to assess the validity of present methods. The load model developed for this research together with the distribution grid model of a sample residential complex with integrated PV systems are combined in a unique simulation tool that is used to investigate power quality factors pertaining to voltage regulation, unbalance and harmonic emissions. The simulation model can also be used to investigate dynamic stability and the voltage and current transient response to various network disturbances. The research builds on the work done in preparation of the NRS 097:2014 specification. The proposed amendments to various standards and guidelines are in response to short comings identified in the study results.

1.7 OVERVIEW OF STUDY

The study outlined in this dissertation combines the findings of academic research papers, field measurements and power system simulations to test the hypothesis.

Chapter 2: Literature Review

The literature review summarizes selected journal articles and conference proceedings upon which the research in this report follows. The outcome of the literature review is the framework and the methodology of the research. This chapter presents background theory of the power quality aspects, which are investigated in the study, specific to the identified research gap.

Chapter 3: Methods

This chapter outlines the flow of the research process, describing the hypothesis formulation and quantifying the hypothesis. The chapter describes the data collection method including field measurements, a survey and the theoretical background of the study methods. The experimental study phase of the research is described which consists of compiling a simulation case file based on the collected data.

Chapter 4: Results

The outcome of the research is published in the results chapter. The results of the simulation study are compared to the quantitative criteria identified in Chapter 3.
The summary in this chapter provides the substantiating evidence required to assess whether the objectives of the research are met and answers the research questions in qualitative terms.

Chapter 5: Discussion

The chapter discusses the parameters under which the hypothesis is valid. The discussion chapter contains an objective interpretation of the results and provides predictions applicable to non-specific study cases based on extrapolation and assumptions.

Chapter 6: Conclusion

The conclusion contains a summary of the research questions, hypothesis, study and results. The conclusion also contains suggestions for further work to follow on this research.

CHAPTER 2 LITERATURE STUDY

2.1 OVERVIEW

Germany announced the 1000 Roofs program in September 1990. Approximately 2000 individuals were granted permission to install grid connected rooftop Photo Voltaic (PV) systems. The aim of the 1000 Roofs program was to investigate the operational behaviour of grid connected embedded generation and to optimize the system components involved [1]. Since then, most international electricity utilities operating in first world countries have drafted integration guidelines for embedded generation in their distribution networks.

Each electrical utility obeys a grid code by which the electrical network is developed, operated and maintained. When comparing the rules and guidelines pertaining to distribution network planning and development, it is evident that each utility uses a grid and load model representing the electricity consumer typical to the respective demographic. The Grid Interconnection of Embedded Generation specification, NRS 097-2-3:2014 [2], focusses on utility connection criteria of small-scale embedded generation in low voltage distribution grids. The NRS 097 standard has been developed to serve as guideline for distribution operators when assessing applications to connect small scale embedded generators. The basis for the calculations of the simplified connection criteria are based on the best practice adopted by utilities of other countries. The specification notes that the technical criteria contained in the document should be enhanced and revised by performing more detailed studies.

The suburban environment in South Africa has changed since the year 2000. Many residential housing complexes are being developed where once larger single houses or smallholdings were found. In [3] it is reported that the number of houses registered in estates grew at an annual average of 30% from 5500 per year in 2000 to 28000 new registrations in 2007. As there are more individual residences per area in estates or

complexes, the concentration of energy consumption has also increased at a similar rate. It is evident that the technical criteria contained in the standards pertaining to typical Low Voltage (LV) networks in South Africa may not necessarily be applicable to distribution grids connecting high density residential complexes with high levels of embedded generation.

Several planning and design criteria place constraints on the capacity of embedded generation in distribution networks [4]. The study presented in this dissertation is based on a 400 V distribution grid of a 45 unit complex connected to an 11 kV grid through a 200 kVA transformer. The study investigates the interaction between an MV equivalent grid, the distribution cable network, a pad-mounted 200 kVA transformer, domestic loads and the embedded PV generation systems. It assesses how inverter connected PV embedded generation affects the following power quality related aspects:

1. Voltage regulation
2. Unbalance
3. Harmonic voltage and current emissions

The result of the simulation study is used to evaluate the planning and compatibility levels contained in the South African power quality standards are exceeded under increasing penetration levels of embedded generation. The compatibility levels are part of the power equipment design standards according to which transformers and cables are manufactured. When power quality compatibility levels are exceeded in practice, the equipment life expectancy reduces as losses and operating temperature increase [5].

2.2 POWER QUALITY CHALLENGES

The following sections summarise the theoretical background of the power quality challenges that will be faced due to increasing penetration levels of embedded generation in low voltage residential distribution networks and the methods of identifying and mitigating these challenges.

2.2.1 Impact of Embedded Generation on Steady State conditions

Steady state is a theoretical concept defined as a snapshot of a network wherein all voltages and load flows remain stable and constant. The snapshot is used as a simulation

base case to evaluate the network dynamic or transient response to disturbances of any sort. With increasing penetration levels of embedded generation, the load profile of distribution grids is set to evolve [6]. Load flow is no longer unidirectional from grid to load as increasing embedded generation capacities allow the consumer become the independent power producer. With many of the renewable energy sources, such as wind turbine generators, run-of-river hydro schemes and PV systems, the availability or load factor of the embedded generation is inconsistent and depends on environmental factors making it difficult to regulate the load flow.

The voltage drop in a distribution grid between the point of supply or the point of connection and the load is due to the load current through the line or cable impedance. An increase in load current increases the voltage drop [7]. Conversely, the voltage at the load increases when the current reduces. The planning guidelines in NRS 034 [8] also address the subject of voltage regulation in grids with embedded generation. Small scale devices with generation capacities less than 13.8 kVA are not required to regulate the voltage at the point of connection [9]. The tap changers of substation distribution transformers are the only devices that can regulate the downstream grid voltage in a residential distribution grid. A changing embedded generation output alters the load flow in the distribution grid, resulting in voltage variations in LV grids that cannot be controlled by the network operator [7]. In the case of small scale PV systems distributed throughout a residential grid, the voltage variation is small compared to the abrupt changes due to loads switching on or off. The solar irradiation changes slowly [10] compared to the instantaneous voltage jumps due to a loads switching and residential circuit breakers tripping. The resulting slow change in system voltage at the point of supply can therefore be regulated by the tap changer of substation distribution transformer similar to the regulation performed during the daily grid loading profile. PV inverters are designed to remain grid connected and operational when the power quality of the grid remains within the compliance limits. If the frequency was to exceed the required limit, all grid connected PV inverters would trip simultaneously resulting in an abrupt voltage change due to the change in load current in the distribution grid. The voltage regulation is one of the study themes investigated in the simulation network.

Current and voltage unbalance is another steady state measure that is impacted by the integration of single phase embedded generation. The unbalance associated with multiple single phase embedded generators can be approximated with the algorithm developed in [11]. The planning guidelines stipulate that single phase embedded generation should be balanced across all three phases to minimize the unbalance at the common distribution transformer. The limit for unbalance on distribution level is 3% [2]. Unbalance causes circulating currents in delta transformer windings increasing losses and operating temperature and reducing the expected life cycle [12]. The voltage unbalance measured on the LV transformer terminal is a function of the load current unbalance and the short circuit level. The measured voltage unbalance is therefore not always a sufficient measure of the detrimental effect of current unbalance in a transformer. The distribution transformers usually have a delta connected MV winding with a high negative phase sequence reactance preventing the unbalance on the LV grid to mitigate to the MV network. Voltage unbalance on the MV terminals is therefore around 5 times smaller than the unbalance measured on the LV terminals.

In the case of high density residential clusters, it is not possible to ensure that the single phase embedded PV generation is perfectly balanced across the three phases. The simulation study investigates various scenarios of short circuit level, embedded generation penetration level and network loading. For the unbalance simulation, it is assumed that all embedded generation is connected the same phase.

2.2.2 Impact of Embedded Generation on background harmonics

Harmonic voltages and currents result from non-linear loads such as switch-mode devices or static power converters connected to a power system. Any given voltage or current waveform can be dissected into its constituent harmonics by means of the Fourier transform. Although magnitudes and angles can be calculated for all frequency sinusoids, for regulation purposes and to increase measurement speed the sinusoidal constituents are calculated as integral multiples of the fundamental frequency by means of discreet Fourier Transform [13]. Different types of loads and switch-mode power supplies and inverters add or subtract from the harmonic spectrum prevalent in a power system. Even transformers are also known to emit certain harmonics in the saturation region of the

magnetic hysteresis curve if poorly designed [14]. The criteria for harmonic voltages and currents contained in the various standards are usually divided into the following three categories:

1. Odd harmonics
2. Even harmonics
3. Inter-harmonics

The odd harmonics are most prevalent in power systems as they are produced by full-wave inverters, rectifiers and other non-linear loads. The odd harmonics that are multiples of three are classified as zero-sequence harmonics that cancel in transformer delta windings in balanced three-phase systems [13]. The even harmonics are DC harmonics produced by half wave rectifiers, which are not implemented in typical electronic domestic loads. The positive and negative half cycles are different in magnitude resulting in a DC component that can cause transformers to saturate.

When new devices, such as PV inverters, are connected to a power system the authority responsible for the power quality in the network assesses how the existing network is impacted. The network development guidelines state planning levels that are to be used in an apportionment of the available margin to ensure that the limits remain within the power quality criteria. The margins and apportionment levels of harmonic voltages and currents contained in the various standards were compiled before the widespread integration of inverter based embedded generation, especially on distribution level. The NRS 097 uses the principle employed on transmission level to place constraints on harmonic emission levels injected by equipment [2]. Harmonic voltage and current phase angles are not addressed in any of the power quality standards. It is therefore not possible to assess compliance with the harmonic current emission criteria of several devices operating in parallel. If the phase angle of an emitted harmonic is shifted 180° from the same harmonic in the background harmonic spectrum, the current at respective harmonic is absorbed by the device. The magnitude of the resulting current vector may exceed the apportionment limit even when the direction of the current is from the grid into the device [15].

The harmonic voltage limits pertaining to the integration of small scale embedded generation fall into the category where harmonic emissions are deemed insignificant. From a regulatory point of view it becomes very difficult to hold individuals accountable for the

harmonic emissions when several embedded generators connect to the same point of coupling. The maximum penetration level of embedded generation connecting to a common feeder inadvertently limits the combined harmonic emissions of several grid connected PV systems. In addition, multiple independent grid connected inverters partially cancel harmonic voltages and currents of each other due to changing phase angles of the respective harmonics. The apportioning method in the IEC 61000 standard applies a diversification factor of 0.5 to the apportionment limits where more than 4 independent inverters are connected [4].

The integration of switch-mode devices on transmission level requires a study of the harmonic impedance of the network. Line and shunt capacitance resonates with line reactance resulting in parallel and series resonance points on the impedance curve at various frequencies [16]. If a non-linear load or switch-mode device emits a certain harmonic current at the frequency where a parallel resonance occurs, it can be expected that the harmonic voltage at that frequency would be magnified, depending on magnitudes and harmonic phase angles. If a voltage harmonic emitted by a device occurs at a frequency of a series resonance in the impedance, the respective harmonic current would be magnified [16]. On distribution level, the cable and line capacitance is very low as capacitance is a function of the voltage squared. The resulting harmonic impedance is therefore predominantly inductive, the impedance increasing linearly as a function of frequency. Without any series and parallel resonance points in the harmonic impedance voltage or current magnification due to resonances is not expected.

The current and voltage harmonic emissions contained in inverter datasheets are determined under ideal conditions. When these inverters connect to a grid with a short circuit level up to 1000 times greater than the load impedance, the actual harmonic currents emitted are much greater and depend on the grid impedance and the existing background harmonics and the respective phase angles [17].

The PV inverters considered in this research employ L-C type filters to attenuate the switching harmonics and reduce the harmonic emissions below the apportionment limits. The L-C filter introduces a parallel and series resonance on the harmonic impedance at the natural frequency of the filter. When calculating the harmonic impedance of the grid at the point of connection the resonance points due to the L-C filter shift to lower frequencies,

depending on the cable impedance between the filter and the calculation point. When harmonic currents resonate with the parallel resonance of the impedance, the resulting voltage may exceed the limit, while the source of the emissions remains within the limits [16].

All equipment is designed to accommodate adverse power quality in terms of harmonics, unbalance and over-voltages and overloading according to the power quality criteria. When harmonic limits used in the equipment design are exceeded, equipment losses and operating temperatures increase resulting in shorter life cycles [18].

2.2.3 Impact of Embedded Generation on System Stability

Stability challenges will arise with increasing penetration levels of embedded generation in distribution grids as voltage and load flow is controlled by several devices [19, 20]. The distribution grid voltage is affected by the control systems of the inverters controlling the PV power flow. The model of the PV system and the control strategy proposed in [21] will form the basis of the simulation model of the individual PV systems in the simulations investigating the voltage regulation, unbalance and harmonic emissions impact on the residential distribution grid. The need for reactive power control and voltage support of the embedded generation for the overall robustness of the distribution grid is addressed in [11]. Poor voltage stability causes additional stresses on the distribution transformers. Smaller pole and pad mounted distribution transformers typically do not have tap changers. The substation transformers converting transmission voltages to distribution levels usually have On Load Tap Changers (OLTCs). With widespread implementation of embedded generation in larger distribution networks these transformers compensate for the varying voltage according to [22], which in turn may interact with the voltage control loop of the inverters of the PV systems leading to instability. The power control in a micro grid with distributed generation requires a power control strategy that can prevent coupling between active and reactive power [23]. Although the voltage and power control methods described in the existing research can provide better network controllability, security and efficiency as a whole, they are not yet implementable in practice as there are no standards, communication protocols and regional controllers specified. There are also no criteria listed in the planning guidelines pertaining to control response and function.

Small grids and PV systems can be represented by transfer functions that can be solved to determine critical gains and time constants before the system becomes unstable. The transfer function of the PV panel, the MPPT and an inverter are derived from [21]. Since the control functions of the various inverters are unique to the manufacturer, general assumptions would have to be made to investigate the effect of high penetration levels of embedded PV generation on the network stability. Since the current planning guidelines and standards have no quantifiable stability criteria, the investigation of the effect penetration level and inverter control response is omitted from this dissertation.

CHAPTER 3 METHODS

The study presented in this dissertation combines various research methods and tools to arrive at a conclusion that proves the hypothesis. This section details the steps followed in the research process. The process of the research is depicted in the flow diagram in Figure 3.1.

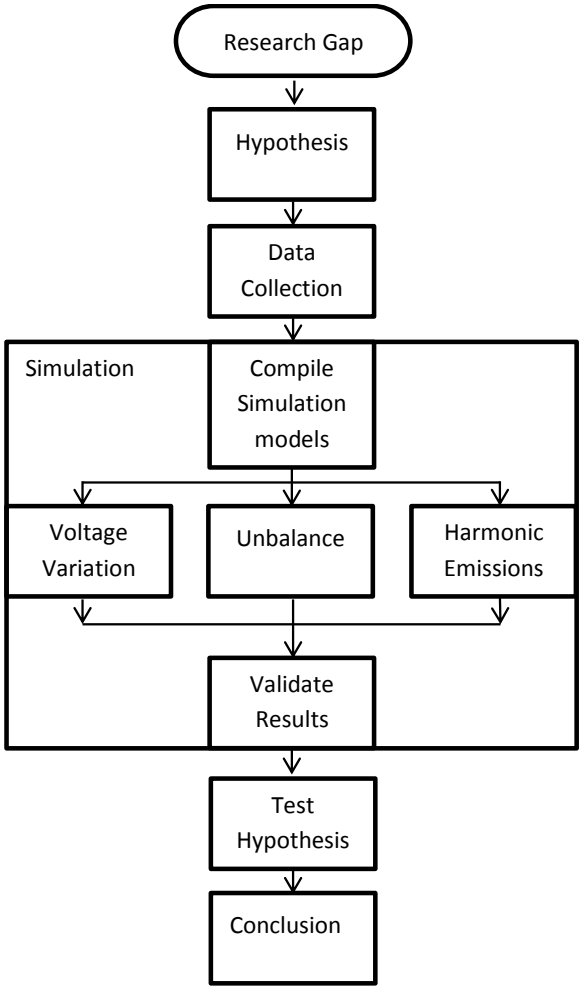

Figure 3.1. Research flow diagram.

3.1 HYPOTHESIS FORMULATION

It has been identified that the failure rate of transmission system equipment has accelerated since the advent of the widespread integration of commercial PV plants into the national grid, especially in locations where several PV plants are in close proximity to one another. The question arose whether the power quality challenges leading to the failures of the transmission level equipment in the PV plants will cause similar failures in distribution equipment when the penetration level of embedded small scale PV generation increases in low voltage distribution grids. This question is translated into the hypothesis that planning guidelines and equipment design criteria have to be revisited to ensure that the future grid can withstand the additional stresses due to the integration of small scale PV distributed generation. The focus of the research presented in this dissertation falls on South African equipment standards and planning guidelines relating to the distribution grid in high density residential clusters integrating grid connect rooftop PV systems.

The essence of the hypothesis is quantified by the power quality limits taken from various local and international standards in terms of current, voltage and frequency characteristics of electricity grids. Each grid, be it an industrial plant, a distribution network, islanded grids or the national transmission networks, is operated according to a set of guidelines. Similar to the operational codes, grids are developed and expanded according to planning guidelines with respect to predicted population growth, economic climate, political climate and climate change [8]. Electricity grid characteristics that fall under the umbrella of power quality include steady state load flow, frequency and voltage response, network transient response and harmonic emissions. A technique to evaluate power quality with weighting factors assigned to various power quality components is proposed in [25]. The weighting factors are chosen subjectively, which will not hold up when disputes surrounding power quality problems arise. A good summary of power quality standards and how power quality aspects are caused and mitigated is presented in [26]. Voltage sags and harmonic emissions are the most widespread power quality challenges. The power quality standards serve as the basic requirements to equipment design standards and network development and planning guidelines. A selection of the most commonly encountered power quality aspects is included in this research. Power quality aspects surrounding grounding,

protection and device specific control features are excluded as they are not quantifiable. The South African standards were chosen to be the principal standards to which the study results are compared.

3.2 DATA COLLECTION

This section describes the different methods that were employed to gather and process the input to the research and study. An engineering-oriented approach is followed to evaluate a distribution network simulation model of a high density residential housing clusters against a practical cluster distribution grid connected to the South African network.

3.2.1 Measurement and Survey

The load model that has been compiled for the simulations in this research had to be verified. For this purpose a power quality recorder was installed at a residential complex consisting of 80 units in the east of Pretoria, South Africa. An ImpedoDuo power quality recorder from CTLab was set up to record three phase voltages and currents on the LV incomer to the complex. The recorder measured for 7 consecutive days to get an insight to the daily load profile of a typical high density residential cluster. The recorder stored measurement values in 1 minute intervals. The ImpedoDuo was configured to record minimum, maximum and 95^{th} percentile values of the 1 minute periods from the analogue input channels at a sampling rate of 500 kHz. Since the LV feeder voltage of 400 V is below the ImpedaoGraph 600 V limit, no voltage probes or voltage transformers were required [27]. The current probes were connected to the metering current transformers having 500:1 turns-ratios.

In parallel to the measurement campaign, a survey was conducted to gain insight into the electricity consumption patterns of the residents. The survey in Addendum A asks the survey participants questions regarding their typical daily routine and what appliances are used at what time and for how long. The answered surveys are then processed to establish daily load profiles according to the method described in [6]. The resulting Diversified Maximum Demand of the total complex is used as a peak load case in the simulation study. The survey was conducted in person and no specific participant sampling method was employed. The survey was conducted in a single day, eliminating some of the residents

from the survey who were not home. As the residents exhibit a high gradient of similarity in routine, demographic, and employment class, it was deemed appropriate to generalize the electricity consumption profile of the absent residents. The validity of this approach is measured against the simulation results of a model of the practical grid with a load model compiled from the scaled survey response.

3.2.2 Power Quality Criteria

The simulation model developed for the purpose of this research is required to be versatile so that different aspects pertaining to power quality can be investigated. The quantifiable terms of the power quality standards that are applicable to high density residential complexes are presented in Addendum B.

A qualitative analysis method is implemented to filter the standards that are unambiguous and applicable to the research. The selection process of the criteria deemed applicable is based on experience and the findings of the research summarized in the literature review. The criteria have to be of a nature that can be used to compare the simulation study results in quantifiable terms. To this end, voltage regulation, three-phase unbalance and harmonic emissions are the power quality aspects evaluated in the simulation study. The power quality standards are divided into two categories: Planning levels and compatibility levels. The planning levels are used during the network development stage and have to be complied with when new devices are integrated into the grid. The compatibility levels are related to the equipment design standards. Equipment manufacturers complying with the South African National Standards design their equipment to withstand the compatibility levels, adding some margin to achieve the respective expected equipment life cycles. When planning levels are exceeded due to the integration of new devices, equipment immunity levels are more likely to be exceeded in the future resulting in equipment loss of life.

The compatibility level is defined as the 5% probability of equipment immunity levels being exceeded for 95% of system disturbances. Limits pertaining to current unbalance are not defined in the power quality standards. The NRS 097 standards mentions that small scale embedded generators should not exceed a current THD of 5%.

Table 3.1 NRS 048 power quality planning and compatibility levels [4].

	Planning Level	Compatibility Level
Voltage regulation	3% variation	+/-15% steady state
Voltage unbalance	1.5%	3%
Voltage THD	5%	8% (11% Short term)

The assessment of the power quality levels is performed on a 95^{th} percentile measurement of 10 minute measurement intervals performed over 7 consecutive days [4]. Short term compatibility is determined from 99^{th} percentile measurement of 3 second measurement intervals of a single day.

3.3 SIMULATION MODEL

The simulation model used for the study component of this research is compiled in PSCAD version 4.6. PSCAD was chosen for the simulation component of the research as all the power quality aspects considered can be simulated in a single software package.

PSCAD employs an electro-magnetic transient processing core that solves simulation grids in the frequency domain. The simulation time step is chosen based upon transmission line reflections and switching converter periods. The switching frequency of the PV system inverter is the determining factor of the solution time step period in this research as the short cable sections can be represented by reflection-less pi-models. The simulation model is based on a practical distribution grid specific to South African high density residential clusters. The simulation model consists of the following subsystems:

- Equivalent 11 kV source representing the municipal MV distribution grid with a peak and minimum short circuit impedance.
- Distribution transformer connecting the municipal 11 kV grid and the LV distribution grid in the residential complex.
- A 400 V low voltage cable network representing the distribution grid of the complex.

- Each residential unit consists of a load rated to the diversified maximum demand with a power factor of 0.9. The loads are replaced by harmonic current injecting sources for the harmonic emission simulation.
- The PV system, consisting of solar panels, maximum power point tracker, inverter and controller. The PV systems are replaced by harmonic current injecting sources for the harmonic emission simulation.

The following sections summarise the background theory of the various subsystems.

3.3.1 Distribution Network

The MV distribution grid is estimated by an ideal source with short circuit impedance typical to MV distribution substations. For the study, a maximum short circuit current of 12.7 kA is chosen and a minimum short circuit current of 1.27 kA. The currents translate to a source impedance of 0.5Ω and 5.0 Ω respectively. Both have X/R ratios of 5, which is typical for distribution grids. The planning guideline stipulates that the MV feeder voltage should not vary by more than ±1.5%. A 1.5% voltage drop is experienced by the MV equivalent source when short circuit impedance is 5.0 Ω and the load current is 17.15 A with a power factor of 0.9. For a short circuit level of 0.5 Ω the 1.5% voltage drop occurs when the load current is 190 A with unity power factor.

The voltage drop over the MV and LV distribution grids is the most prominent technical determining factor in the selection of cables and transformers used in the grid development. The NRS 034 distribution planning standard prescribes a maximum voltage drop of 3% over the MV cable or transmission line grid and a maximum of 8% over the LV distributor. Using these two maximums the cables are selected to meet those limits for a given load. The standard cable sizes used in South Africa are listed in Table 3.2. The *R, X* and *B* value are per unitised on an 11 kV voltage and 100 MVA rating. The rated power represents the current maximum continuous current when the cable is operating at 11 kV. The curve in Figure 3.2 depicts the maximum cable length transmitting the rated current while maintaining a voltage drop of 3%. The electrical properties of the cables used in South African distribution grids are manufactured according to the SANS 10142-1:2009 standard. Complying with the standard ensures that all cables of similar type have very similar electrical properties, regardless of manufacturer. The cable properties listed in

Table 3.2 are taken from [59]. The cables referenced are all 11 kV, 3-core, copper conductor, armoured, XLPE type cables with different conductor diameters.

Table 3.2 Electrical properties of 11kV cables [59].

Copper area mm^2	Rated Power MVA	Resistance pu/m	Reactance pu/m	Susceptance pu/km
25	2.50	0.00060	0.00077	0.00782
35	3.05	0.00043	0.00056	0.00873
50	3.77	0.00032	0.00042	0.00965
70	4.57	0.00022	0.00030	0.01078
95	5.37	0.00016	0.00022	0.01214
120	6.10	0.00013	0.00018	0.01341
150	6.82	0.00010	0.00015	0.01431
185	7.72	0.00008	0.00013	0.01565
240	8.80	0.00006	0.00011	0.01744
300	9.68	0.00005	0.00010	0.01938

The cable resistance and reactance decrease with increasing conductor area. As the insulation thickness remains the same for a rated voltage, the ratio between conductor surface area and insulation thickness increases as the conductor size increases, resulting in increasing cable capacitance.

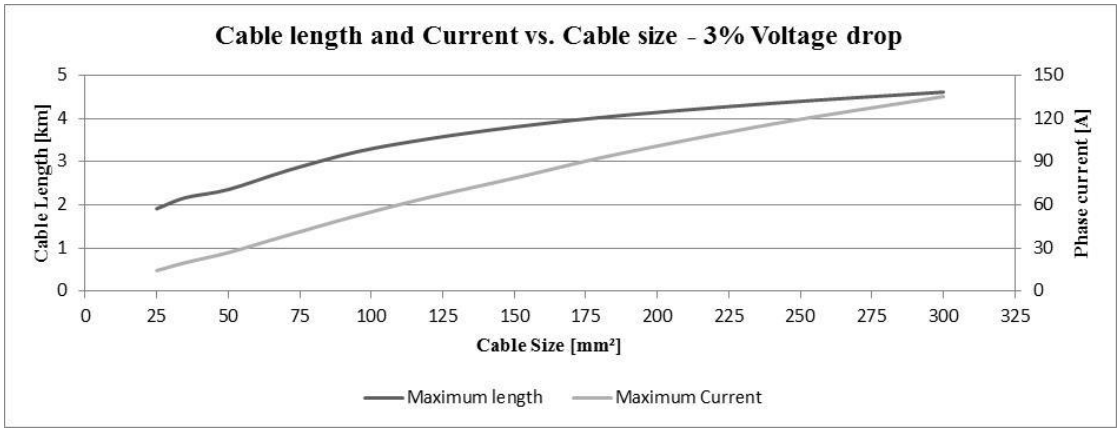

Figure 3.2. 11 kV cable maximum length and current for 3% voltage drop.

If the 11 kV cable was chosen based on the voltage drop alone, the losses would be unfeasible. For a 200 kVA load, the phase current is 10.5 A for an 11 kV three-phase system. A 25mm^2 3-core copper cable can be up to 13.8km long before the voltage drop over the cable reaches 3% for a phase current of 10.5 A.

The *R*, *X* and *B* parameters at 20°C operating temperature, based on a base of 11 kV and 100 MVA are:

$$R = 6.01 \times 10^{-4} pu/m$$
$$X = 7.73 \times 10^{-4} pu/m$$
$$B = 7.82 \times 10^{-3} pu/m$$

The 25 mm^2 buried copper cable has a current rating of 131 A, translating to 2.5 MVA power rating at 11 kV. The voltage drop over the 5 km cable is 0.5% for a loading of 100 kVA and 3% for a current equal to the loading of 630 kVA.

The LV cable distribution networks in high density clusters in South Africa are designed for three units closest to one another sharing an LV three-phase supply. The voltage drop over the cable length has to be less than 10% or 18.47V when the Notified Maximum Demand (NMD) is absorbed by the load. The residential distribution grid considered in this research is designed to allow each residential unit to have an NMD of 13.8 kVA with a circuit breaker rating of 60 A. The LV cable grid has to be rated to facilitate this 60 A current while limiting the voltage drop to 10%. Figure 3.3 shows the voltage drop over the indicated cable length for a 60 A current through the cable. In addition to the peak load

flow rating, various margins and derating factors are applied before the appropriate cable size is determined [8]. The voltage drop is calculated for an operating temperature of 90°C.

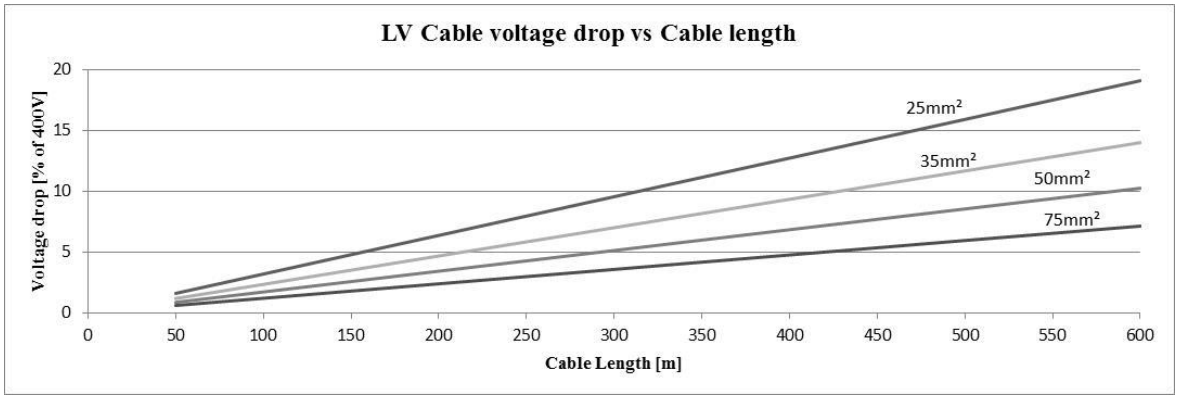

Figure 3.3. LV cable voltage drop vs. cable length.

From Figure 3.3 it can be deduced that cable sections longer than 300m require 35mm² copper cable and sections longer than 400m require 50mm² copper cables to limit the maximum voltage drop to 10%. Aluminium conductors have higher impedance values per cross sectional area of conductor due to the higher resistivity of aluminium compared to copper. The rating principle remains the same. The LV cables used in the simulation network are buried copper 4-core conductors, unarmoured, PVC type. The capacitance value is not provided for LV cables as is considered insignificant in 400 V grids as the capacitance is a function of the voltage squared. The capacitance is calculated with (3.1).

$$C = 1.08\frac{0.024\epsilon_r}{log\left(\frac{GMD}{r}\right)} \quad \mu F/km/phase \tag{3.1}$$

The $log\left(\frac{GMD}{r}\right)$ value for the 35mm^2, 1000V copper cable is 0.009 and the relative permittivity for PVC is $\epsilon_r = 2.2$. For the sake of uniformity, all cables in the simulation network, regardless of length, have 35mm² copper conductors with the following *R*, *X* and *B* parameters:

$$R = 0.3275pu/m$$
$$X = 0.6875pu/m$$
$$B = 2.875 \times 10^{-9}pu/m$$

The base of the per unit impedance is 400 V and 100 MVA.

Harmonic characteristics

Harmonic currents have to be taken into consideration when calculating the cable ratings. Harmonic currents cause eddy currents on the surface of conductors which increase losses [33]. The neutral return is shared by three customers and has to be rated to withstand three-phase unbalance and harmonic currents according to the compliance levels. The neutral conductor may overload when unbalance and harmonic currents exceeds the compliance margins. In such a case, it may be necessary that each phase conductor has a dedicated neutral return conductor. Low voltage cables have very small line charging capacitance values as the capacitance is a function of the voltage squared. Harmonic resonance points between the cable inductance and capacitance are therefore insignificant compared to the resonance between the inverter filters and the line inductance. For the residential grid considered in this research the L-C filter has a typical capacitance of 5µF and the LV cable impedance varies between 0.17mH for a 50m section and 1.40mH for a 400m section of 35mm^2, 4-core copper cable. Applying (3.2), a preliminary series impedance resonance point can be calculated for the LV feeder if the MV grid is not considered.

$$F_{LC} = \frac{1}{2\pi F_0 \sqrt{LC}} \tag{3.2}$$

The resulting series resonance points lie between 1.9 kHz and 5.3 kHz. Series impedance resonance points magnify harmonic currents at the resonance frequency while parallel resonance points tend to magnify the harmonic voltage at the respective resonance frequency. If a switch mode device was to emit harmonic voltages and currents at the frequencies of network impedance resonance points, it may be that the measured harmonics exceed the relevant limits, even if the emission levels of the device are within the apportioned margin.

3.3.2 Distribution Transformer

One of the research objectives is to assess whether the equipment design guidelines used in developing the distribution grids of high density residential areas are sufficient when the penetration level of PV embedded generation reaches 25% of the distribution transformer

kVA rating. The distribution three-phase transformers are delta-wye Dyn11 type transformers with the wye neutral solidly grounded. For complexes housing between 20 and 160 residential units, the standard transformers used in South Africa are presented in Table 3.3. The number of units sharing the transformer has been determined from the Diversified Maximum Demand method using (3.3). The listed transformers are all 11/0.42 kV delta-wye, three phase units. The electrical properties of the transformers are taken from [48]. The SANS 780 standard ensures that these standard transformers are manufactured according to the specifications provided in the standard. The electric characteristics of these transformers are therefore very similar, regardless of manufacturer.

Table 3.3 Standard 11/0.42 kV distribution transformers [48].

TRF Rating [kVA]	Impedance [%]	Load Losses [%]	No Load Loss [%]	# Units sharing
100	4.5	1.70	0.30	24
200	4.5	1.35	0.26	50
315	4.5	1.21	0.23	81
400	4.5	1.13	0.23	104
500	5	1.08	0.22	131
630	5	1.02	0.21	167

The distribution transformer size used in the PSCAD simulation model is based on the 4 kVA diversified maximum demand resulting from the approach described in 3.3.2 [8]. For the 45 Unit cluster considered in this the 11/0.42 kV transformer is rated 200 kVA. The SANS 780 compliant 200 kVA transformer in [48] has No Load Losses (NLL) of 520W, or 0.26% of the rating, full load losses of 2700W, or 1.35%, and an impedance of 4.5%.

The relatively low cost of distribution transformers does not justify specialised grid integration studies to determine whether location specific network conditions and characteristics may affect the transformer life cycle [5]. Only the basic parameters

including transformer kVA rating and the normal operating voltages are used by the grid planners when selecting transformers as the transformer designs should comply with the standard specification and cover most of the typical power quality challenges [49]. The degradation of the insulation is the main cause of premature transformer aging. The degradation of the insulation depends on the thermal characteristic, including operating temperature, ambient temperature and temperature rises due to various losses of the transformer and how the thermal energy is removed by the oil and container [50]. The health of a transformer can be analysed by performing an oil analysis. Oil heating, arcing and corona leave traces of dissolved gasses such as Hydrogen, Carbon Monoxide, Methane, Ethane and Acetylene in the oil, which can be analysed to determine failure mechanism or relative age of the transformer [51]. The loss of life analysis from the oil quality is only applicable if the transformer oil has not changed since manufacture. The loss of life of transformers due to thermal degradation of the insulation material can be mitigated by overrating new distribution transformers taking load unbalance and harmonic emissions into account. References is made to the IEC 60076 standard when stating that distribution transformers are not required to accommodate harmonic currents greater than 5% of the transformer rating [52]. The harmonic emissions cause higher load and no-load losses raising the temperature beyond the life-cycle rating of the insulation. An increase of 6°C operating temperature halves the transformer life cycle [53]. Load unbalance causes a zero sequence path allowing the triplen harmonics to circulate in three winding transformers, further increasing the operating temperature and reducing the life cycle [54]. The K-factor is an optional rating that can be applied to transformers operating in networks with high harmonic emissions. Through special construction, the transformer oil temperature of a K-factor transformer remains lower than a conventional transformer resulting in a longer life cycle.

The loss of life is calculated by applying (3.3), where θ_H is the hotspot temperature.

$$L_{actual} = L_{design} \times 9.8 \times 10^{-18} e^{\left(\frac{15000}{\theta_H + 273}\right)} \tag{3.3}$$

The hotspot temperature is a factor of the harmonic current distortion and the operating temperature. As the transformer loading varies as a function of the demand profile in residential areas, the operating temperature also varies according to the temperature time

coefficient. Since the period during which the transformer is subjected to heavy loading is only short during the evening and morning peak times, the operating temperature of distribution transformers typically remains lower than its full load rating allows. The peak loading of the transformer is only a couple of hours during times when the ambient temperature is also relatively low. The example in [50] is applicable to the transformer used in the study for this dissertation, concluding that temperature rise from increased harmonic emissions associated losses is not significant enough to warrant k-factor transformers in residential grids.

3.3.3 Short Circuit Level calculation

The short circuit level can serve as a good indication of the vulnerability of a grid to power quality challenges. The ratio between short circuit level and loading can be interpreted as a measure of network strength, where a high ratio points to power quality immunity. The short circuit level depends on the impedance between the source of the short circuit current and the point where the short circuit level is calculated. The excerpt of the simulation distribution grid model depicted in Figure 3.4 is used to calculate the short circuit level at the common LV point of connection, at the residential load of a consumer electrically close to the common connection point and a resident electrically far removed.

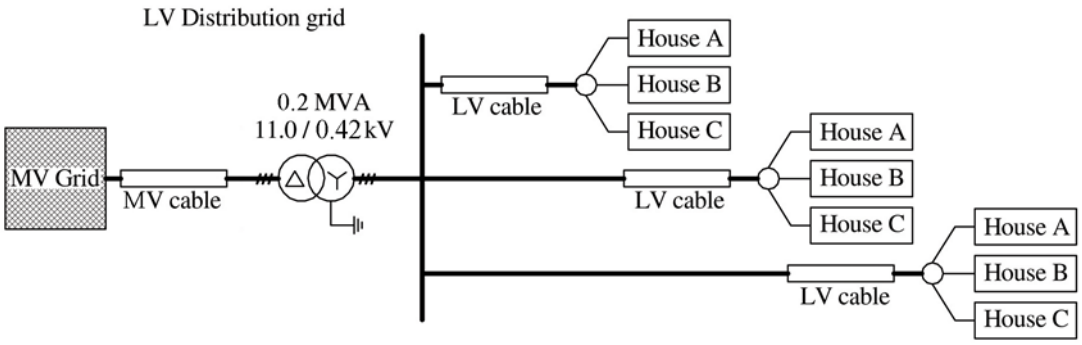

Figure 3.4. Distribution grid simulation model section.

The lengths of the LV cables vary between 50m and 400m. The short circuit level is determined for grids rated according to the number of units listed in Table 3.3. The short circuit current is calculated on the transformer LV terminal and at a residential unit 50m

from the transformer and another unit 400m from the shared feeder. The equivalent source representing the MV distribution grid at the regional substation has a typical peak short circuit level of 242 MVA and a minimum short circuit level of 24.2 MVA.

$$SCL_{TRF,LV} = \frac{0.4^2}{(Z_{TRF}+Z_{SCL,MV})} \tag{3.4}$$

$$SCL_{Load,LV} = \frac{0.4^2}{3(Z_{Cable}+Z_{TRF}+Z_{SCL,MV})} \tag{3.5}$$

As the impedance of the different network components are added in series, the largest impedance tends to dominate the result.

Table 3.4 Distribution grid short circuit levels.

	Minimum MV Short Circuit Level			Peak MV Short Circuit Level		
TRF MVA	TRF LV MVA_{SCL}	Short cable MVA_{SCL}	Long cable MVA_{SCL}	TRF LV MVA_{SCL}	Short cable MVA_{SCL}	Long cable MVA_{SCL}
100	1.815	0.224	0.071	1.954	0.228	0.072
200	3.433	0.272	0.075	3.955	0.277	0.076
315	5.000	0.293	0.077	6.199	0.299	0.077
400	6.007	0.302	0.078	7.829	0.308	0.078
500	6.575	0.306	0.078	8.832	0.314	0.078
630	7.710	0.312	0.078	11.012	0.319	0.079

It is difficult to assess the relative short circuit level from the MVA_{SCL} values in Table 3.4. Figure 3.5 depicts the ratio between the short circuit level and the transformer rating. The ratio depicted in Figure 3.6 is based on the Notified Maximum Demand of 13.8 kVA. These two graphs provide valuable insight to the vulnerability of a distribution network to voltage regulation and unbalance.

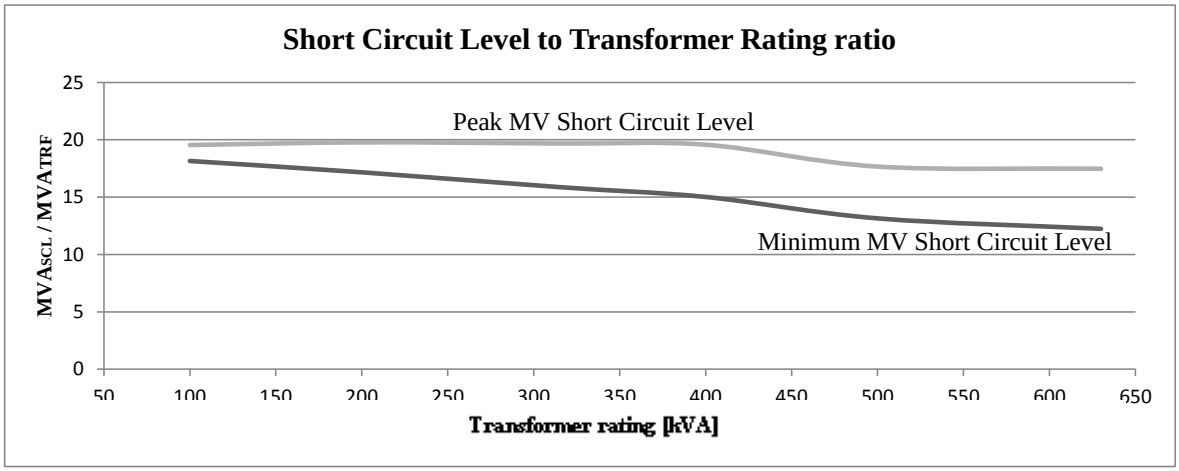

Figure 3.5. Short Circuit Level to Transformer Rating ratio.

As the size of a residential cluster distribution grid increases, the number of units sharing a common feeder increases, resulting in a higher MV/LV distribution transformer rating. The ratio between resulting short circuit level and the demand or the transformer rating decreases as the size of the complex increases. The dip in the two curves between the 400 and 500 kVA transformer in Figure 3.5 is due to the increase in transformer impedance from 4.5% to 5%. This is a design feature of the transformers contained in the South African standards SANS 780.

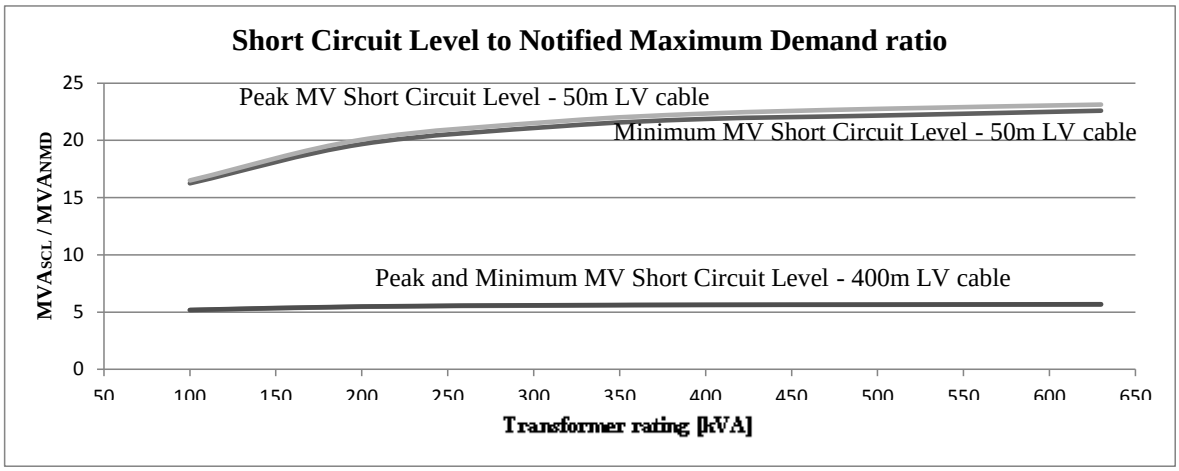

Figure 3.6. Short Circuit Level to NMD ratio for different network sizes.

The cable impedance dominates over changes in short circuit level as the length of the cable approaches 400m as seen in Figure 3.6. The short circuit level remains constant

regardless of changes in MV short circuit level and regardless of the distribution transformer rating. As the cables become shorter, the impact of the short circuit level of the MV grid and the transformer impedance start to affect the ratio between the LV short circuit level and the notified maximum demand.

When the ratio between short circuit level and demand is very low, the point where the ratio is determined is susceptible to voltage variation due to changes in load current. The three-phase unbalance also becomes more prominent when the ratio between short circuit level and transformer rating becomes lower. This is illustrated by the

3.3.4 Load Model

Various publications, research, guidelines, frameworks and standards make use of load models to forecast energy demand, plan new networks, develop and upgrade existing networks in pursuit of greater efficiency and reliability in servicing a changing customer demand profile [28 - 30]. A bottom-up approach similar to the one described in [6] is implemented to develop the simulation model of the residential load model presented in this research. Measurement data compared to simulated results is used to verify the accuracy of the models.

Utilities in South Africa use statistical load data to approximate the diversified maximum demand of different consumer classes. For domestic loads the following assumptions are made [8]:

- Domestic loads can be modelled as currents.
- Loads lie within a positive range of values – between zero and the circuit breaker size.
- When a frequency of occurrence histogram of the load currents is plotted, it is best modelled by a Beta probability density function (pdf).
- The load pdf can be either skewed to the left or right (shape).

Applying these assumptions, a formula is developed to estimate the diversified maximum demand of residential loads where more than 10 consumers are connected to a common Low Voltage (LV) supply.

$$L = 0.23 \times N \times \frac{c}{a+b}\left[a + 1.28\sqrt{\frac{a \times b}{N(a+b+1)}}\right] \quad (3.6)$$

L is the maximum load, N is the number of consumers and a, b and c are model parameters that are calculated from the measured data trend to derive the diversified maximum demand. The diversified maximum demand is used in forecasting load profiles. In the simulation study, the result is used in the sizing and rating calculations for distribution equipment. For the 45 unit complex simulation model used in the study of this research a = 1.42, b = 4.13, and c = 60 resulting in a diversified maximum demand 3.98 kVA per unit used in the 15 year distribution development plan. As the number of units sharing a common transformer increase, the diversified maximum demand decreases as seen in Figure 3.7.

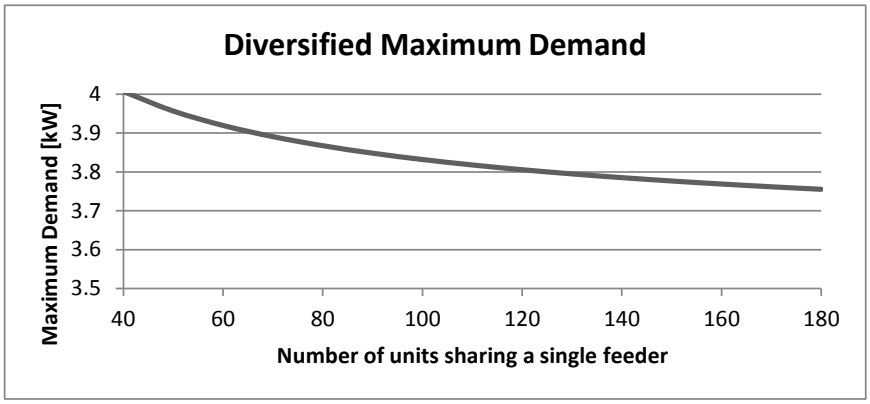

Figure 3.7. Diversified Maximum demand per household in high density complex.

The short circuit breaker rating is assumed to be 60A resulting in a Notified Maximum Demand (NMD) of 13.8 kVA per unit [2]. A shortcoming of this approach is that the equation relies on historical measurement data processed to apply to a certain demographic. Electricity consumer behaviour and community habits are constantly evolving as cities grow and the economic environment changes [24]. Energy efficient appliances are also more predominant. It becomes very difficult to predict consumer profiles for future network planning and design. A further challenge lies in the measurement technique itself. The sample intervals should be as short as possible to prevent statistical smoothing of the measured data trends [31]. Short sample intervals on the other hand result in vast amounts of data. The daily load profile in Figure 3.8 is the winter and summer load profile of middle income residential consumers. Enerweb compiled the load profiles from 618 million recording taken over a 10 year period from

1994 until 2004 [56]. The recorded data was processed and filtered for residential electricity consumers with a household income of R10000 per month. The data is therefore applicable to the middle income households of the consumers living in high density residential clusters considered in this dissertation. The standard deviation of the load profiles is 0.5 kVA. The peak in the winter profile in Figure 3.8 of 5.8 kVA is 45% greater than the calculated diversified maximum demand of 3.98kVA.

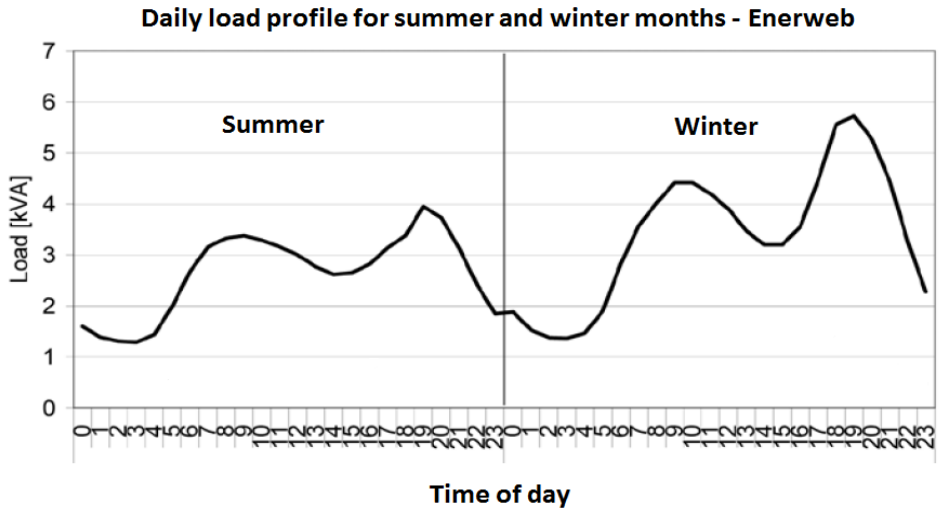

Figure 3.8. Load profile of middle income consumers, taken from [56] with permission.

From energy recordings taken at a 20 unit residential cluster the daily demand profile in Figure 3.9 was compiled. The recordings span from the 1st of January 2015 until the middle October 2015. The summer months are considered to be January, February and March and the winter months are June, July and August. From within these two periods the weekday demand data was filtered and normalised on a per consumer basis.

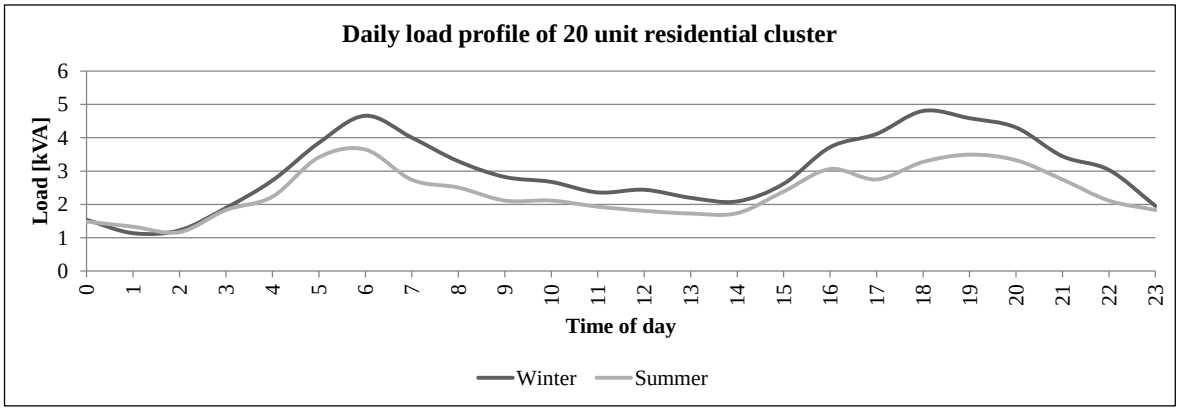

Figure 3.9. Weekday load profile of a 20 unit residential cluster.

The winter peak of 4.8 kVA is only 20% larger than the calculated maximum diversified demand. Compared to the 5.8 kVA winter peak in Figure 3.8, the 20 unit winter peak is 20% smaller. There are a couple of reasons for the larger diversified demand in Figure 3.8:

- The recordings are based on household income criteria and include consumer living in full title stand houses with higher auxiliary power requirements such as swimming pools and external lighting.
- The domestic appliances and lighting solutions in 1994 – 2004 were not as energy efficient as in 2015.

The winter peak demand is between 35% and 45% higher than the summer peak demand.

The discrepancy between the peak demand magnitudes in the profiles in Figure 3.8 and Figure 3.9 motivate the development of an application specific load model that can be customised to a specific demographic. With the advent of urbanization, the number of high density complexes connecting to MV distribution grids has increased at an astonishing rate [3]. Some MV distribution rings consist of 100% high density residential clusters. Distribution equipment including cables and transformers have to be rated to take the demand profile specific to high density clusters into account. This is one application of the load model developed in this research.

The simulation model of the load is a composite model of domestic appliances. The power ratings of typical appliances in Table 3.5 are taken from the research published in [32].

Table 3.5 Typical power and energy ratings of domestic appliances.

Appliance	Power Rating	Daily usage
Geyser	2600 W	3 hrs.
Stove	3000 W	1.5 hrs.
Kettle	2000 W	0.3 hrs.
Fridge	160 W	5 hrs.
Other	1200 W	1 hrs.
Electronics	100 W	24 hrs.
Heating	1200 W	4 hrs.

The research survey in Addendum A was compiled to determine time of use information of the appliances used most commonly by the residents by means of ratio-scale questions. The duration of use and the time that each appliance is in service depends on each individual household. Since most of the residents in the complex have similar working hours and habits, the respective times are quite similar and can be grouped as depicted in Figure 3.10.

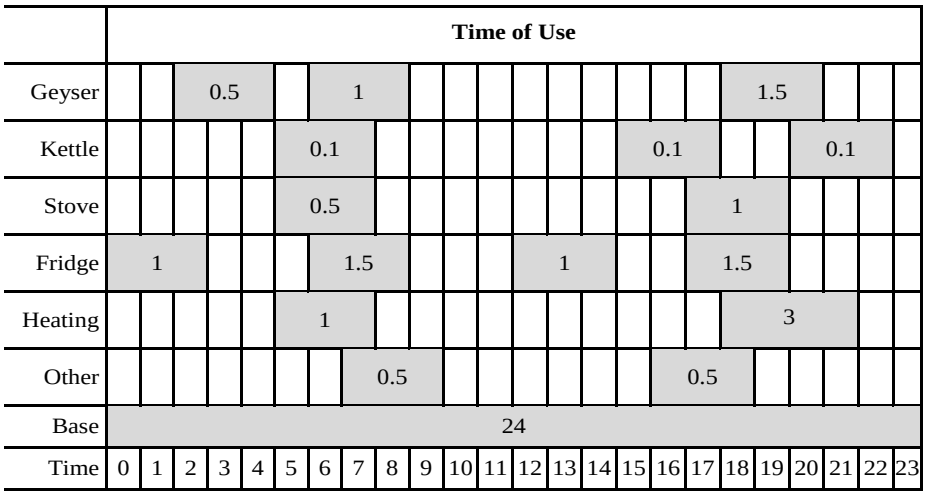

Figure 3.10. Time of use sumary of typical household appliances.

The grey areas in Figure 3.10 indicate the times during which the appliances are in operation for the duration, in hours, indicated by the number in the respective areas. The base-load of electronic equipment is in service at all times and represents the standby power of various appliances as well as computers, power supplies and other entertainment systems. CFL and LED lights also make use of rectifiers. The time-of-use data is added to the simulation model as independent loads that can be switched according to a random function with normal distribution. A daily load profile is created by repeating the 24 hour simulation several times until a normal distribution with confidence of 90% is reached. The resulting daily load profile of a 45 unit high density residential complex is depicted in Figure 3.11. From the peak 90% confidence value the simulated diversified maximum demand is calculated as 4.1 kVA for the summer demand peak and 4.9 kVA for the winter peak. The measured 95th percentile peak consumption of the 80 unit complex upon which the load model is based was 279 kVA which translates to a diversified maximum demand of 3.49 kVA per unit.

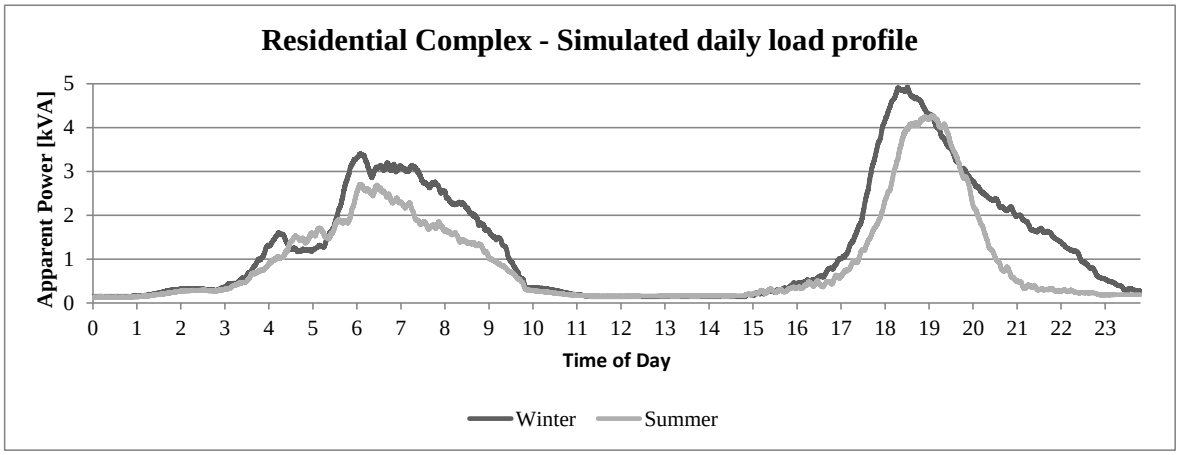

Figure 3.11. Simulated daily load profile of a 45 unit complex.

Since the measurement was conducted in September 2015, during two weeks of moderate temperature, it is assumed that the measured diversified demand is representative of the summer profile. With the winter peak demand around 40% higher than the summer demand, it can be deduced that the diversified maximum demand would be around 4.9 kVA when space heating is added [34]. The diversified maximum demand calculated with (3.3) is 3.98 kVA for a 45 unit complex and 3.86 kVA for an 80 unit complex. The

simulation, the measurement data and the calculation method result in a similar diversified maximum demand for a summer load. The winter load is however around 40% greater than the summer demand. Following the trend of improving energy efficiency in home insulation, appliances and lighting, it can be argued that the demand profile will not increase in the foreseeable future, unless a disruptive technology, like electric vehicles, is adopted [35]. When such an abrupt change in demand takes place, the calculation method will have to be completely rethought. Although the adoption of a new technology, like electric cars, will be gradual, the impact of a few charging stations within a complex will have a substantial impact on the demand profile. The rate of the charging will depend on regulations and circuit breaker ratings, but it can be expected that the fast charge cycle will cause the households considered in this research to meet the notified maximum demand of 13.8 kVA. Scheduled charging will have to be adopted to prevent equipment ratings being exceeded [57]. There are several scenarios that would have to be considered when including this technology in the planning and rating calculations. With so many theories and unknowns, the impact of electrical vehicles on the distribution grid has not been included in this research.

Table 3.6 Diversified Demand summary.

	20 Units	80 Units	From [56]	45 Units	45 Units
	Measured	Measured	Measured	Calculated	Simulated
Winter max	4.8 kVA	-	5.8 kVA	4.0 kVA	4.9 kVA
Summer max	3.6 kVA	3.5 kVA	4.0 kVA	4.0 kVA	4.1 kVA
Winter min	1.0 kVA	-	1.3 kVA	-	0.3 kVA
Summer min	1.1 kVA	0.8 kVA	1.3 kVA	-	0.3 kVA

Appliances which are predominantly resistive or constant impedance loads, such as water and space heaters and ovens, stoves and kettles, draw current that is voltage dependant. During brown outs and voltage dips on the distribution grid these loads reduce in power consumption thereby assisting the network with the recovery. Electronic loads require constant power, even during times of lower voltage. The load current increases inversely to

the fall in voltage to maintain a near constant power resulting in a prolonged low voltage recovery period after voltage dips. The effect of prolonged under-voltages on various appliances was investigated by the Power Systems Engineering Research Centre and published in [36]. Appliances powered by induction machines such as fridges and air conditioners are even more susceptible to voltage sags. When the voltage falls the induction motors decelerate. If directly connected induction machines decelerate pas the critical slip, the motors tend to stall. As soon as the voltage returns the motors accelerate drawing current that is similar in magnitude to the starting current which is up to six times the rated current. Being mostly inductive during start-up, the motors tend to depress the voltage during the recovery period after a network event, causing under-voltage relays to trip if the penetration level of induction motors is relatively large compared to the short circuit level [24].

The load model used in the peak load simulation study is represented by a 4 kVA series R-L load with a power factor of 0.9 [37]. The minimum load model is a 2 kVA series R-L load with power factor 0.9.

Harmonic characteristics of domestic appliance loads

Thermal loads including geyser, kettle, air conditioning and hair dryers are typically the most power intensive domestic appliance loads. When observed from the shared feeder of the complex, the diversified load profile during peak consumption times consists 95% of constant impedance loads and induction machine loads and 5% of electronic loads. During off-peak times in the late evenings, the electronic loads account for 20% of the combined minimum load. All electronic loads employ rectifiers and DC-DC converters to produce stable DC voltages required by the electronic systems. Full wave rectifiers inject harmonic currents into the AC grid, manifesting themselves in the 3^{rd}, 5^{th} 7^{th} harmonic in decreasing magnitude [38]. The wave-shape of different type of loads varies as a function of the DC current drawn by the respective appliance. The University of Wollongong in Australia published a laboratory research paper on harmonic measurements of various modern day appliances. The current harmonic values in Addendum C, Table C.1 are the measurement results of the research published in [15]. Each harmonic current and voltage is

characterised by magnitude, frequency and phase angle in relation to the fundamental frequency voltage waveform.

Since the phase angles of the harmonic currents are functions of the load current, duty cycle and switching frequency of switch-mode power supplies, the various appliance harmonic currents add and subtract according to magnitude and phase angle. The currents should be multiplied by a diversity factor that depends on the number of appliances in service [39]. The same approach is followed to calculate the diversity factor of loads in a given residential complex. Since the fundamental current of electronic appliances is usually relatively low compared to the thermal devices like geysers and space heating and air conditioning, with power ratings 10 to 100 times greater than the electronic loads, the harmonic currents in terms of amperes RMS are still relatively low during times of peak consumption.

3.3.5 PV system

Small scale renewable energy producers most commonly employ rooftop PV systems as these are relatively inexpensive and easy to install and operate compared to other renewable energy generators such as wind turbines and fuel cells. Inverter datasheets are vague concerning the harmonic emissions and control parameters. The emission data used in this dissertation is therefore based on laboratory results from [17]. Typical small scale inverters are designed to emit a Total Harmonic Distortion (THD) of less than 5.0%, where

$$\mathrm{V}_{THD} = \frac{\sqrt{V_2^2 + V_3^2 + V_4^2 + \cdots + V_n^2}}{V_1} \tag{3.7}$$

$$\mathrm{I}_{THD} = \frac{\sqrt{I_2^2 + I_3^2 + I_4^2 + \cdots + I_n^2}}{I_1} \tag{3.8}$$

When new devices, including power plants, dynamic reactive power compensators, large motor drives and rectifiers are integrated into the MV, HV and EHV transmission grids, a harmonic apportionment is performed. Existing background harmonics are measured and subtracted from the planning limit resulting in a margin that is then apportioned according to a standard specific formula. Any new plant has to comply with the harmonic current and voltage apportionment requirements before being deemed grid code compliant [4].

On distribution level, in residential areas especially, this approach is not followed. The compliance level of the Total Harmonic Distortion of distribution equipment is 8%, which from a historic point of view, gives sufficient margin for harmonic distortion due to rectifier loads and other loads emitting non-sinusoidal waveforms. The planning guidelines classify small scale PV inverters as Stage 1 devices having to comply with very basic apportionment requirements [2]. When proposing non-specific compliance requirements such as these, the equipment standards have to be well coordinated with the planning guidelines to provide sufficient margin covering the uncertainty pertaining to the integration of unknown devices.

PV Panels

The daily solar irradiation profile is influenced by location and season. The change in irradiation due to weather and cloud cover is in a time frame of one second to several minutes compared to the dynamic response of the electrical network which is typically less than 100 ms. The PV panels can thus be represented by a constant current source in parallel with a diode and a resistor as shown in Figure 3.12 [40].

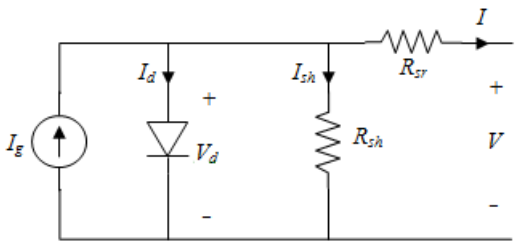

Figure 3.12. PV panel electrical equivalent model.

The output current and voltages of the PV panel are determined by applying (3.7).

$$I = I_g - I_d - I_{sh} \tag{3.9}$$

$$I_{sh} = \frac{V + IR_{ST}}{R_{sh}} \tag{3.10}$$

$$I_g = I_{SC}\frac{G}{G_R}[1 + \propto_T (T_c - T_{cR})] \tag{3.11}$$

G_R and T_{cR} are the reference solar irradiation and reference cell temperature respectively. $\propto_T$ is the temperature coefficient which is typically around 0.0017A/K for silicone cells. I_{SC} is the short circuit current of the cell.

$$I_d = I_o \left[exp\left(\frac{V+IR_{ST}}{nkT_c/q}\right) - 1 \right] \tag{3.12}$$

$I_o$is referred to as the saturation current, n is the diode ideality factor, k the Boltzmann constant and q the electron charge. n = 1.3 for silicon cells. The saturation current is dependent on the cell temperature according to (3.11).

$$I_o = I_{oR} \left(\frac{T_c}{T_{cR}}\right)^3 exp\left[\left(\frac{1}{T_{cR}} - \frac{1}{T_c}\right)\frac{qe_{g\prime}}{nk}\right] \tag{3.13}$$

$e_{g\prime}$ is the band-gap energy of the solar cell material. The series and shunt resistor values R_{ST} and R_{sh} can be determined by an iterative process.

The V - I curves in Figure 3.13 and Figure 3.14 show the effect of solar irradiation and cell temperature on the output of the solar panel.

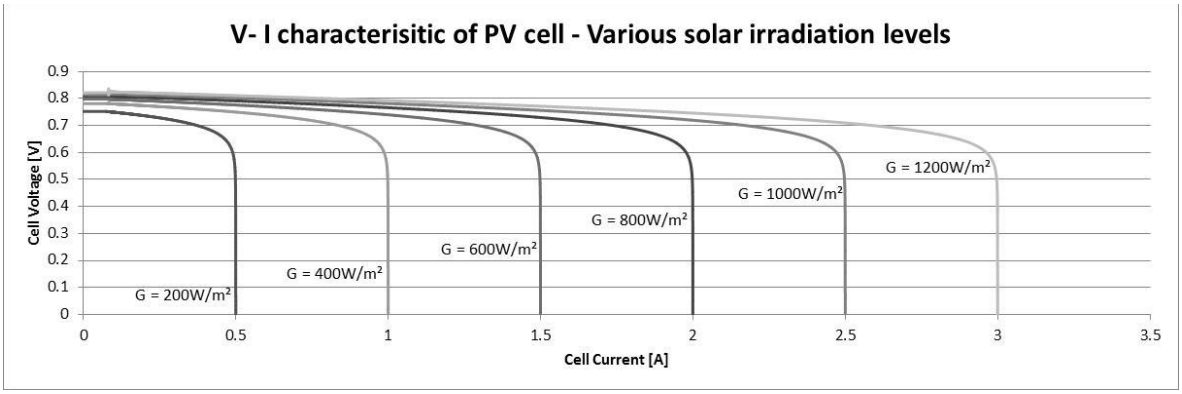

Figure 3.13. PV panel V-I characterisitic – Effect of solar irradiation.

The relationship between the reduction in solar irradiation and the cell current is linear. The knee-point voltage remains constant, but the open circuit voltage decreases with the reduction in solar irradiation.

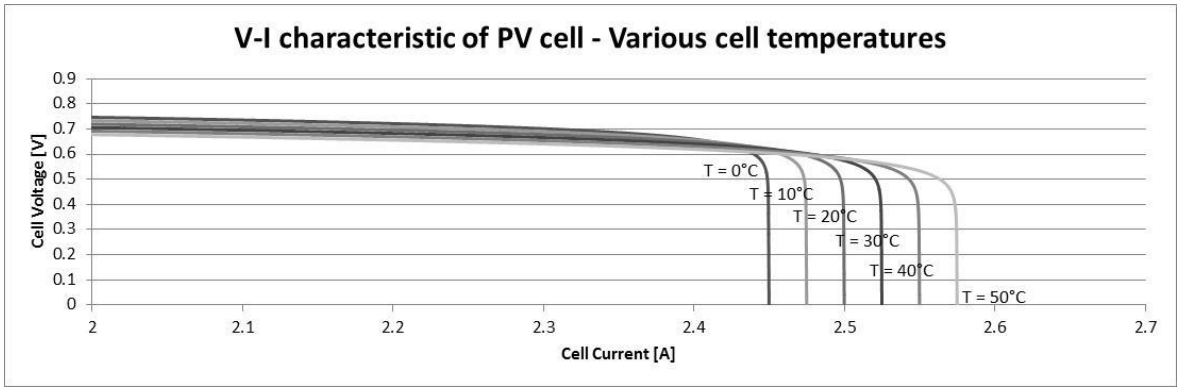

Figure 3.14. PV panel V-I characterisitic – Effect of cell temperature.

An increase in cell temperature allows for higher short circuit currents, but as the knee-point voltage reduces, the resulting output power also reduces. The knee-point in Figure 3.13 and Figure 3.14 represents the maximum power point which is tracked by a Maximum Power Point Tracker (MPPT). An MPPT is in essence a DC-DC converter optimising the cell voltage-current ratio by chopping the current, allowing the cell to operate close to the knee-point [41]. The maximum power point is affected by temperature and irradiation levels as depicted in Figure 3.15. The maximum output power reduces by 0.2% per 1 C increase in cell temperature. The maximum output power increases by 0.16% per 1 W/m² increase in solar irradiation.

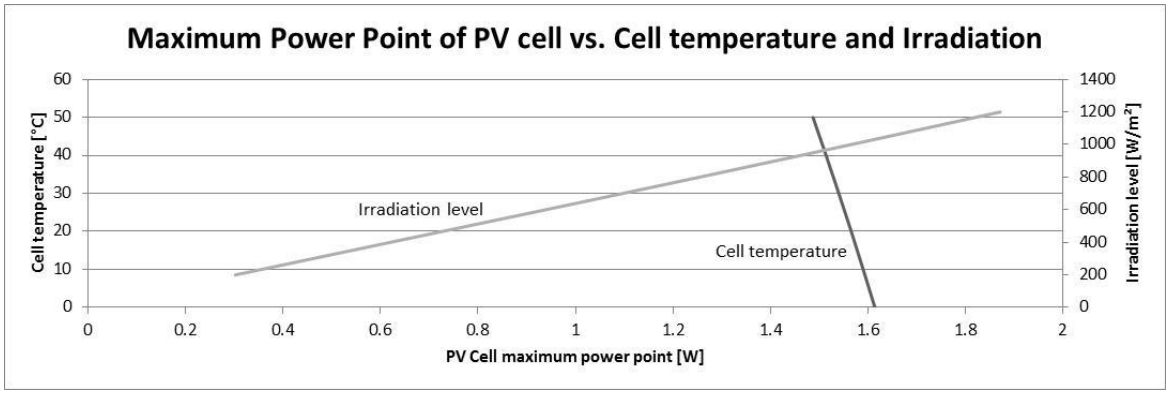

Figure 3.15. Solar irradiation and cell temperature vs. PV panel maximum power.

When PV panels are connected in series and the irradiation levels of the panels differ, it is possible for more than a single maximum power point to exist as described in [42]. In practice this effect becomes more pronounced during the twilight times in the mornings

and evenings. Multiple maximum power points can create instabilities in the maximum power point tracker as the algorithm follows different points on the V-I curve. When the ambient irradiation tends towards a minimum threshold, the cell voltage starts to change rapidly. During times of low irradiation, the output voltage becomes unstable, which could lead to grid instabilities if the embedded generation penetration level is very high [43].

Maximum Power Point Tracker

The maximum power point tracker is the interface between the PV panels and the inverter. It is mainly required to optimize the PV output power under changing load currents. From the PV curves in Figure 3.13 it can be seen that the cell voltage falls rapidly as the load current increases. Since the output power is directly proportional to voltage and current, it is important to maintain both at optimal levels. A secondary function of the MPPT is to track the maximum power output under changing irradiation levels and cell temperature.
There are 4 standard types of maximum power point tracking algorithms [41]:

1. Constant Voltage Tracking (CVT)
2. Perturbation and Observation Method (P&O)
3. Incremental Conductance Method
4. Gradient variable step long admittance incremental Method

The PSCAD model used in the simulation study employs the P&O method. This is a very simple and robust tracking method that applies a small perturbation on the PV voltage and measures the resulting current to determine the output power. If the power is higher than before the perturbation, the voltage is adjusted to the perturbation level. This process is repeated to find the knee-point voltage where the power is the highest and a steady state is reached. The MPPT voltage continues to oscillate around the knee-point [10]. In this study a simple DC-DC boost converter is used to vary the PV DC voltage to maintain the maximum output power. The PSCAD model MPPT tracker used in the study is depicted in Figure 3.16.

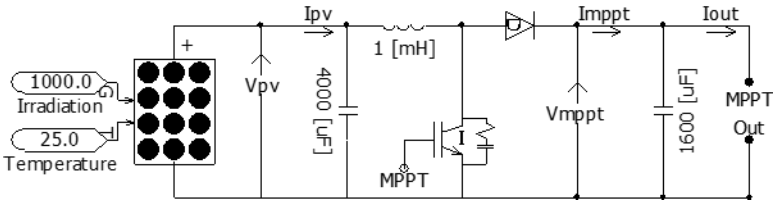

Figure 3.16. Simulation model of MPPT tracker and DC-DC boost converter.

The switching frequency of the DC-DC converter was chosen to be 2 kHz. The switching frequency is usually chosen to minimise losses of the converter while maintaining the output voltage and current ripple below a desired level. In this case, the simulation time-step becomes the constraint to the switching frequency. Through a trial and error process it was found that a switching frequency of 2 kHz provides accurate results without causing the simulation time to become extensively long.

Using the approach described in [44], the DC-DC boost converter component values for a 4 kW system are calculated. The DC-link capacitor C_{DC} is a function of the output ripple requirements of both, the boost converter and the inverter. Equation (3.12) does not take the inverter effect into account. C_{DC} is refined using the simulation to obtain a harmonic emission spectrum corresponding to a practical system.

$$C_{DC} = \frac{P\ D_{max}}{V_{DC} f_{sw} \Delta V_{DC}} \tag{3.14}$$

The boost converter output power is assumed to be equal to the inverter output power $P = 4000W$. The DC-DC boost converter output voltage V_{DC_Avg} is 115% of the peak output voltage equal to 375.6V as this represents the highest peak steady state voltage that the inverter can be subjected to continuously in a distribution grid. ΔV_{DC} = 3.75V and the largest Duty Ratio $D_{max} = 0.6$. The boost converter inductor is calculated with (3.13)

$$L_{DC} = \frac{D_{max}[V_{DC}(1-D_{max})]^2}{2Pf_{sw}} \tag{3.15}$$

The DC link capacitor $C_{DC} = 1600\mu F$ and $L_{DC} \approx 1.0mH$. The PV panel capacitor was chosen to be $C_{PV} = 4000\mu F$ which is 2.5 times C_{DC} [21].

The controller of the DC-DC boost converter is depicted in Figure 3.17. The Maximum Power Point Tracking algorithm is a standard PSCAD component employing the P&O tracking algorithm to determine the maximum power point voltage. The voltage error between the maximum power voltage and the actual PV output voltage is integrated by the

PI transfer function with a gain of 0.1 and a time constant of 50ms. The duty cycle *D* is limited between 0.1 and 0.6 as these values result in the required DC voltage range for which the lowest modulation variation is required by the inverter under varying load conditions. The filtered output power signal of the DC-DC boost converter is used as the power reference to the input to the final integrator. The comparator builds the firing pulse train for the IGBT by comparing the control signal to the triangular wave.

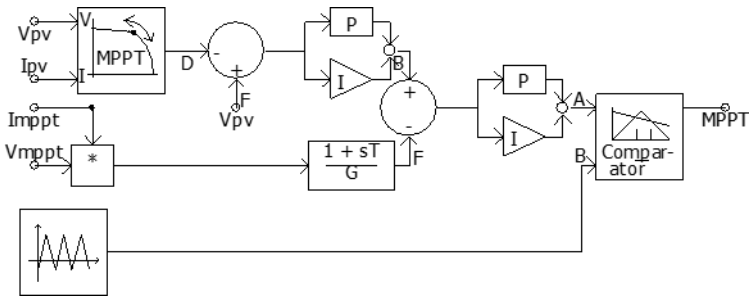

Figure 3.17. Control function of MPPT tracker and DC-DC boost converter.

The simulation results indicate that the PV output power remains constant under changing load resistance and linear under changing solar irradiation.

Figure 3.18a) depicts the DC-DC boost converter power response to changing load current and Figure 3.18b) is the power response to changing irradiation levels. The boost converter response is compared to the PV panel output to highlight the advantage of employing an MPPT system.

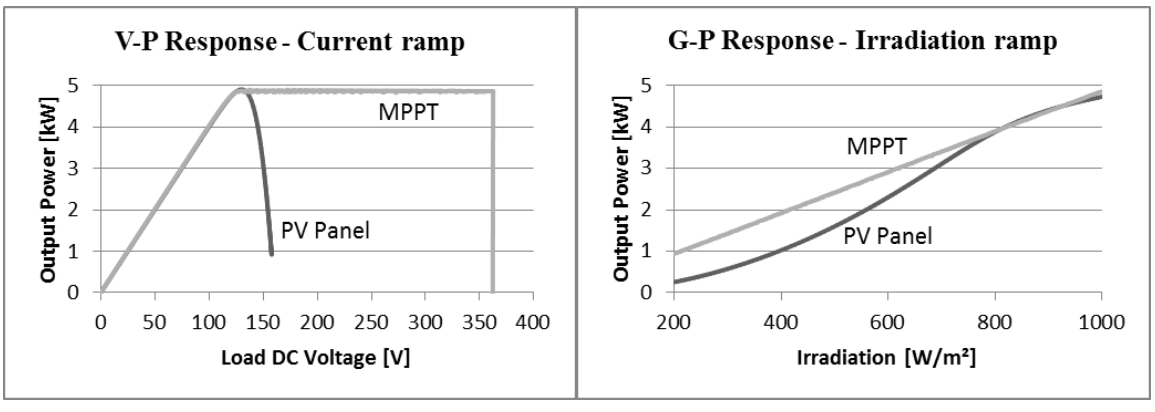

(a) (b)

Figure 3.18. Boost converter output power response to (a) load current and (b) irradiation level.

Inverter Model

The crux of the PV system is the inverter. The inverter consists of a Voltage Source Converter (VSC) and an L-C filter [21]. The inverter model considered is developed for small scale, single phase systems connected to distribution grids. There are however different inverter topologies for both single and three-phase systems. The requirement of the inverter model used in this dissertation is to represent practical inverters in terms of dynamic behaviour, transient response and harmonic emissions.

According to the South African Grid Code for small-scale renewable energy power plants connected to the grid with a power output of up to 13.8 kVA, inverter connected plants have to control the voltage in such a way that no reactive power is injected into the distribution network. Reactive power may only be absorbed to a limit where the power factor remains above 0.9 [2]. The inverter considered in this study follows the network voltage to maintain the reactive power output at zero during steady state operation. In [21] the H-Bridge is controlled by a rotating reference frame or DQ-control to produce a voltage waveform equal in magnitude to the system voltage at the point where the inverter connects to the grid. In essence, the phase angle is adjusted to control the active power and the reactive power output is maintained at zero by controlling the voltage waveform magnitude. The L-C filter affects the dynamic characteristic of the inverter system as the filter inductor acts as a delay function. Before the control algorithm can be developed, the harmonic design has to be completed to size the filter components required as input to the control algorithm.

One of the constraints of the PSCAD model is the switching frequency. The simulation of the simple distribution grid becomes very cumbersome when several inverter PV systems are used, as the high switching frequency reduces the simulation speed. To overcome this while maintaining sound numerical stability in the PSCAD simulation, the switching frequency of the inverter was chosen to be 5 kHz. The resulting inverter, together with MPPT tracker and DC-DC boost converter is depicted in Figure 3.19.

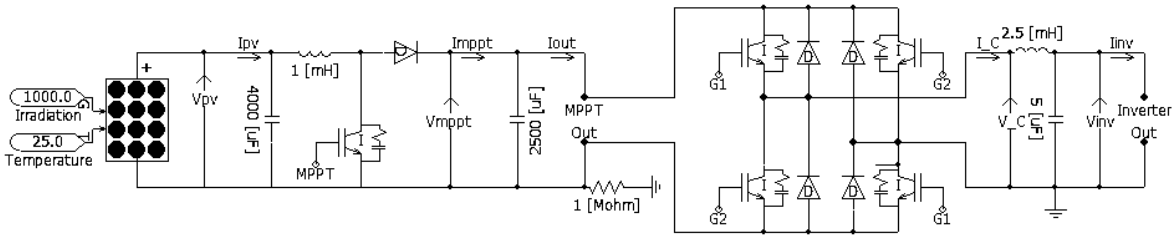

Figure 3.19. Complete PV system single line diagram.

The control circuit for the inverter uses the grid voltage signal as reference frequency, phase and magnitude. The active power is controlled by controlling the phase of the voltage of the VSC waveform and the reactive power is controlled by adjusting the magnitude. The magnitude also has, to a lesser extent, an impact on the active power through the L-C filter inductor and the phase also affects the reactive power through the same coupling mechanism. This current-impedance relationship of the inductor is also incorporated in the control function. The control algorithms of the inverter developed in [21] takes the gains and time constants of the transfer functions of the PV panels, the MPPT tracker, DC-DC converter and inverter into consideration to ensure that the resulting output remains stable when connected to a network.

To attain a similar harmonic current emission profile to the practical inverter for the frequencies below 1500 Hz, the L-C filter values and the DC link capacitor were adjusted until the profile matched relatively well for the lower order harmonics. Current distortion due to the grid connected inverter has to remain below the limits stipulated in [4]. The H-bridge inverter consists of four IGBTs with freewheeling diodes in parallel. The resulting harmonic emission is calculated by the same approach followed in [45]. The L-C filter connected on the AC side of the H-bridge reduces the switching harmonics. The purpose of this study is to assess practical limitations to the penetration level of the inverter based PV systems in an LV grid. It is therefore required that the harmonic emissions reflect practical values. The LC-filter parameters are determined using a trial and error process by adjusting the inductance and capacitance until the harmonic currents match those of a typical PV inverter while the inverter is connected to a resistive 4.0 kW load. Harmonic analysis performed in PSCAD is compared to the harmonic currents from a practical inverter in Figure 3.20. The practical model harmonic current values are exerts from [46].

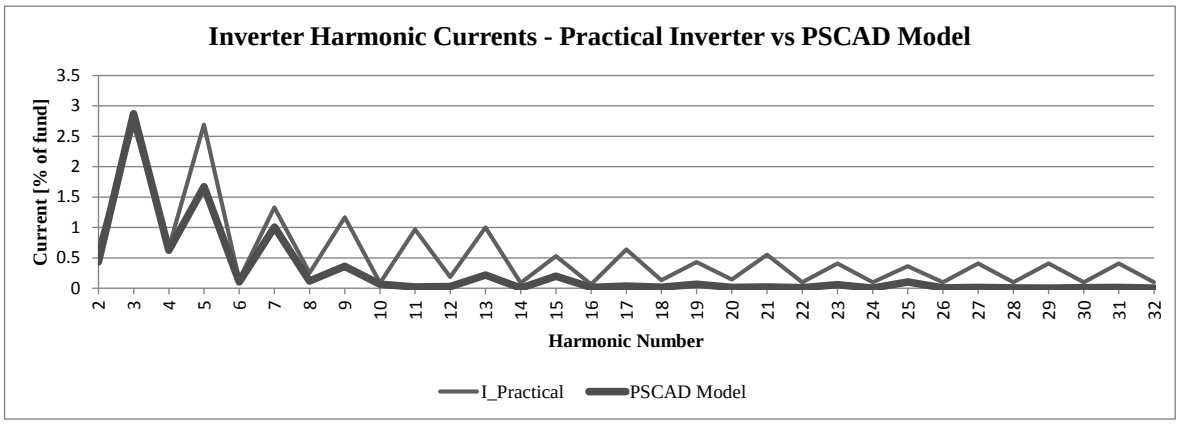

Figure 3.20. Inverter harmonic currents – Practical inverter vs. Simulation model.

The simulated harmonic currents follow a similar trend to those of the practical PV inverter. The even harmonic magnitudes match within an acceptable margin of error. The odd harmonics of the higher order frequencies differ significantly. The error is attributed to the L-C filter which differs from the practical model to facilitate the lower switching frequency.

The inverter harmonics vary as a function of the output power and grid voltage. In the simulation model used in this dissertation it is assumed that the PV inverter system power output is always as high as the solar irradiation allows. Figure 3.21 depicts the magnitudes of the 3^{rd}, 5^{th} and 7^{th} harmonic current emitted by the simulation model while the solar irradiation is ramped from $1000W/m^2$ to $400W/m^2$. For this simulation, the inverter is connected to an ideal source with a short circuit level of 600 kVA. The short circuit level is approximated from the measurements comparing a change in load current and a change in voltage [47]. The maximum 3^{rd}, 5^{th} and 7^{th} harmonic currents emitted by the inverter are between 6 and 15 times larger than the magnitude stated by the inverter manufacturer when connected to the grid under reduced irradiation levels. The harmonic currents at a power output of 4 kW correspond to the inverter manufacturer stated emissions.

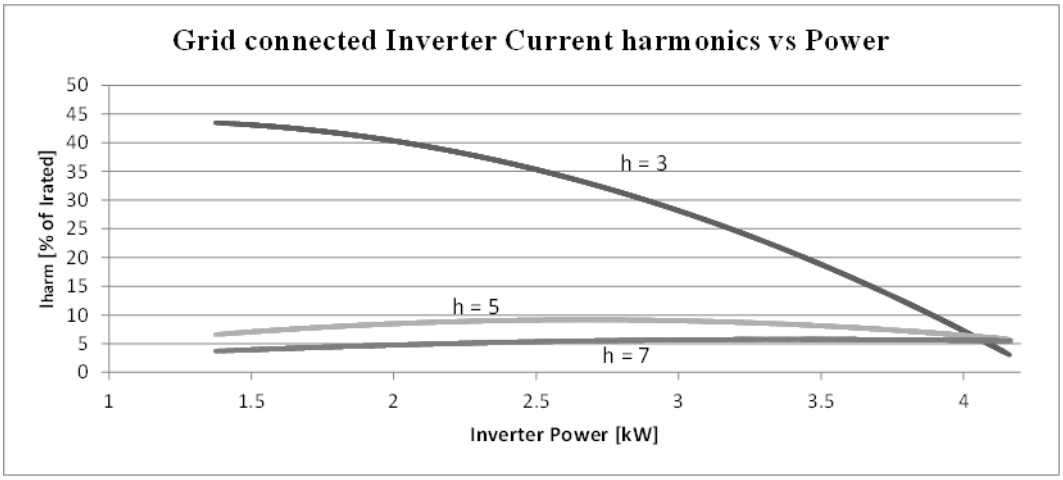

Figure 3.21. Inverter current harmonics vs. output power.

These maximum currents are used in the harmonic current injection simulation as they represent a viable scenario that is encountered daily during the twilight periods. Under reduced output, the emissions of the inverter exceed the limits for the 3rd, 5th and 7th harmonic current for small scale generation which are 4% per harmonic as outlined in NRS 097-2-1.

The controller developed for the PSCAD model is based on the DQ-controller in [21] and is depicted in Figure 3.22.

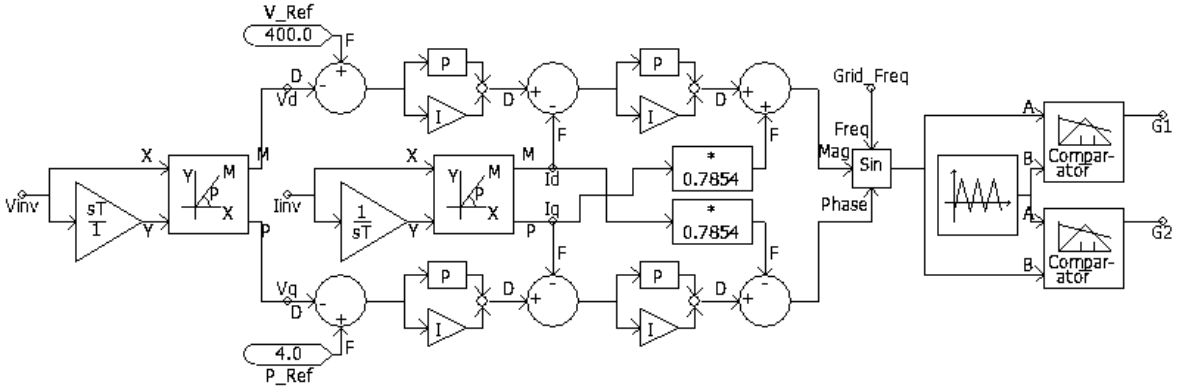

Figure 3.22. Inverter DQ-controller.

After integrating five inverters to the simulation grid, it was found that the inverters would become unstable as the P-I controller gains were determined with only one inverter in a relatively strong network. With several inverters controlling power flow and voltage, the

transfer function of the grid in combination with the inverters became underdamped. As there are no dynamic criteria listed in the standards and planning guidelines, the topic of the dynamic response is not relevant to this research. The switching characteristic of the inverter remains important as harmonic emissions are a function of the duty cycle and the switching current magnitude. The controller can therefore be approximated from a steady state set-point calculation. The requirements of the grid connected inverters are to export the rated power with a power factor as close to unity as possible. This requirement is translated to an active power reference of 4 kW, depending on the solar irradiation, with a reactive power set-point of zero. The resulting controller is depicted in Figure 3.23.

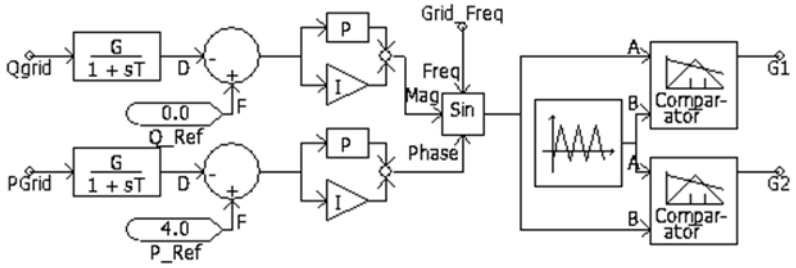

Figure 3.23. Simplified steady state inverter controller.

The first low-pass filter has a gain of 1 and a time constant of 0.1 seconds to remove any ripples from the measurement signal. The PI transfer function of the reactive power has a gain of 20 and time constants of 0.1 second. The PI transfer function of the active power has a gain of 200 and time constants of 0.1 second. These gains were determined by trial and error to ensure that the exported active and reactive power of all connected inverters stabilize within 1 second from the start of the simulation while remaining stable.

3.4 SIMULATION STUDY

A deterministic approach is followed in the simulation study, comparing penetration level of embedded generation to the quantified power quality limits. The study employs the PSCAD simulation model that was developed for the purpose of this research. The simulation model represents a practical high density residential 400 V distribution network connecting to the municipal 11 kV grid via a single 3-phase transformer. The simulation study consists of sections addressing voltage regulation, three-phase unbalance and harmonic emissions respectively.

The other power quality aspects including grounding, protection and control requirements are project specific and manufacturer dependent. The requirements are difficult to translate into quantitative terms that can be analysed in a simulation and for that reason they are omitted from the research study.

3.4.1 Voltage Regulation simulation method

The voltage regulation study uses the NRS 097 3% voltage variation limit as evaluation criteria. The voltage varies as a function of the distribution system loading and short circuit levels as well as on the voltage control performed by the embedded generation. It is assumed that the inverters do not perform active power control beyond evacuating the rated output under irradiation level of 1000W/m² and cell temperature of 25°C. The reactive power output is maintained at zero VARs during steady state. The resulting voltage variation measured at the transformer LV winding is therefore only a function of the load size and the short circuit level, the output power of the combined embedded generation and the cable network impedance. Approximating these by a simplified balanced three-phase model of a MV cable, transformer and LV distribution grid load with power factor of 0.9, a relationship between short circuit level and voltage variation can be established. The load is sized according to the transformer kVA rating. The voltage variation is initiated by disconnecting 25% of the load. The resulting voltage variation magnitude is plotted against complex size in terms of transformer rating.

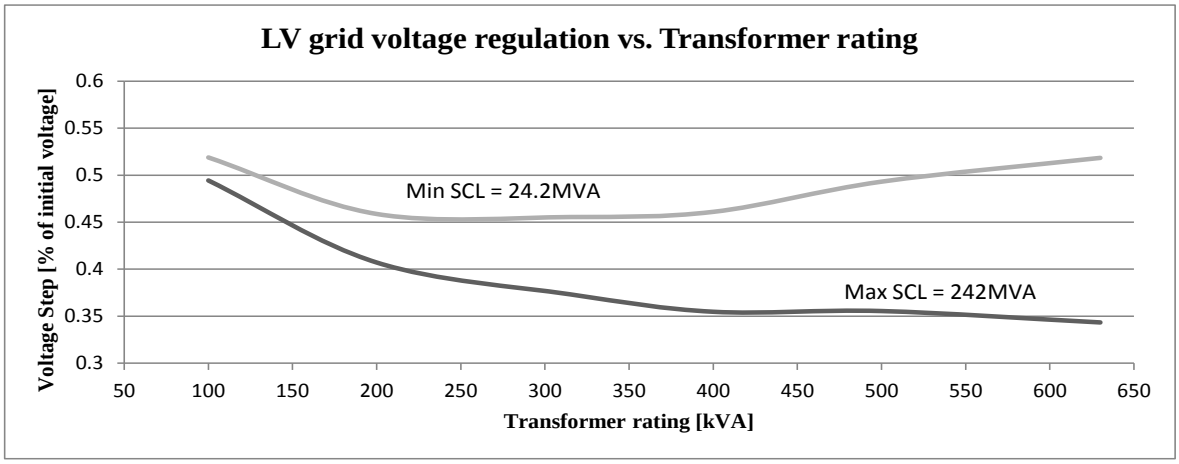

Figure 3.24. LV grid voltage regulation as function of transformer rating.

The magnitude of the voltage variation in Figure 3.24 is a function of the short circuit level on the MV grid and the transformer impedance. The transformer impedance of larger rated transformers becomes relatively larger, while the MV grid impedance remains the same. Under the minimum short circuit level the transformer impedance becomes the determining factor as the transformer rating increases. The area between the maximum and minimum short circuit level curves can be considered to represent the expected voltage regulation for a 25% change in loading. Figure 3.24 can therefore be used to estimate the voltage regulation range for various transformer ratings or LV grid sizes.

The voltage regulation magnitude on the MV terminal of the transformer is shown in Figure 3.25.

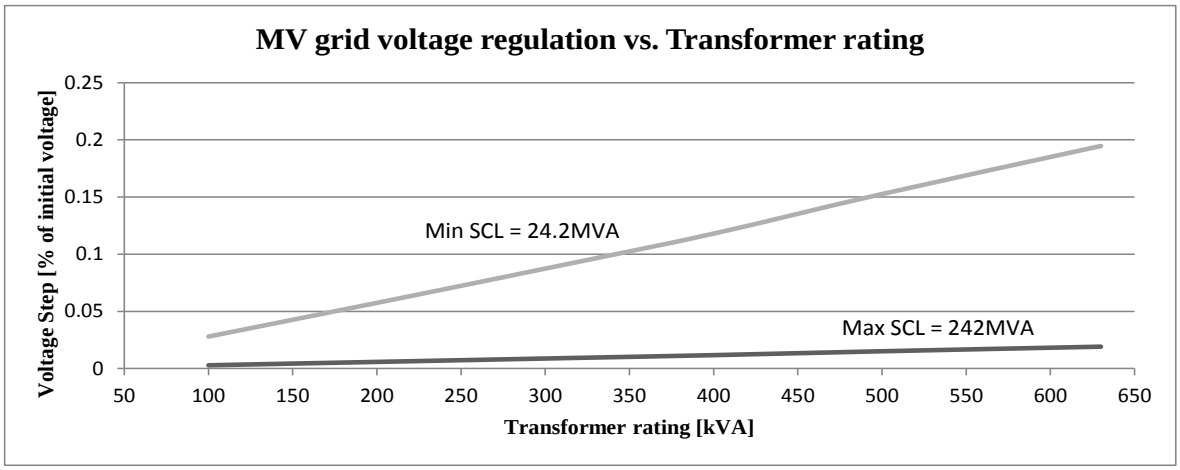

Figure 3.25. MV grid voltage regulation as function of transformer rating.

The MV voltage variation is much smaller than that of the LV grid as the transformer impedance does not play a significant role in the voltage regulation of the MV grid. The voltage regulation in the MV grid is a factor of the short circuit level and the 11 kV cable impedance and surge impedance loading.

In the simulation study the voltage regulation in response to various penetration levels of embedded generation is also investigated. The estimated results are determined by adding loads with different percentage of the transformer rating to the LV side of the transformer. Before the load is added, the transformer is loaded 50%, supplying a constant impedance load with power factor 0.9.

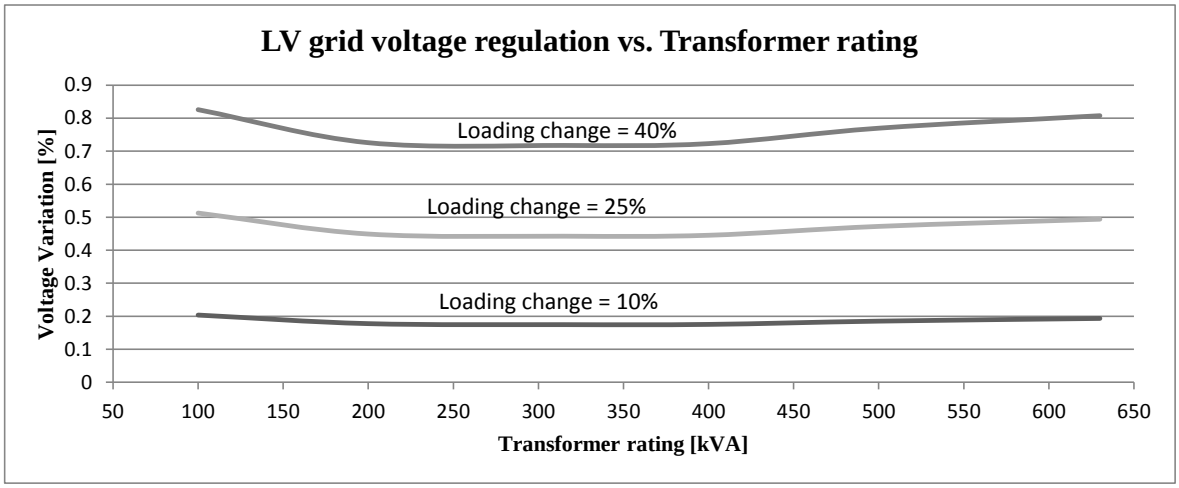

Figure 3.26. LV voltage regulation as function of loading change and transformer rating.

The magnitude of the voltage variation increases as a result of the magnitude of the loading change. The increase in voltage variation between the 10% and the 25% change in loading is ~150%, regardless of transformer rating. The change between the 25% and 40% change results in an increase of ~60% of the voltage variation, regardless of the transformer rating. The non-linearity of the voltage variation lines is due to the transformer impedance. The voltage variation in all of the preliminary calculations remains below the 3% margin of the NRS 097 standard. The results from Figure 3.24, Figure 3.25 and Figure 3.26 are used to validate the results from the PSCAD simulation of a detailed LV distribution grid.

Since most of the large power consuming loads are constant impedance loads, the load current is affected by the magnitude of the voltage at the load terminals. With various cable lengths between the transformer LV terminals and the single phase loads, the voltage variation calculation of the entire grid becomes complicated prompting the use of the PSCAD simulation tool. The positive sequence voltage of the transformer LV winding is recorded under increasing penetration levels of PV embedded generation. Each of the cases is simulated with the system load equal to the notified maximum demand as well as the scenario when the total complex load is 45% of the transformer rating. The following cases are considered to be the determining scenarios:

Case 1: PV generation is 10% of transformer rating

Case 2: PV generation is 25% of transformer rating

Case 3: PV generation is 40% of transformer rating

Simulation parameters

Loads 1: 45 units each with a 4 kVA load with power factor 0.9, resulting in a peak load current which is 90% of the transformer rating.

Loads 2: 45 units each with a 2 kVA load with power factor 0.9, resulting in a minimum load current equivalent to 45% of the transformer rating.

- PV system: maximum power of 4 kW with zero VAr output control
- Three phase maximum short circuit level at the transformer LV winding: 3.7 MVA
- Three phase minimum short circuit level at the transformer LV winding: 3.2 MVA

The 200 kVA distribution transformer impedance dominates over the 11 kV short circuit level. The 11 kV short circuit level has to be reduced by a factor of 10 to reduce the 400 V short circuit level at the transformer windings by 15%. The residential units incorporating embedded generation are randomly selected, but the single phase generators are connected to balance the three phases.

3.4.2 Unbalance simulation method

The voltage unbalance in a distribution network of a high density residential complex follows a similar profile to that of the daily load profile when no embedded generation is considered. The unbalance can also be approximated by a diversification calculation

similar to (3.4) which is used to calculate a load diversified maximum demand. As of yet, there is no diversification equation for the voltage or current unbalance included in the South African planning guidelines. For this reason, the empirical load model used to determine the daily load profile in Figure 3.11 is used in PSCAD to simulate the unbalance for various grid sizes in the form of daily unbalance profiles for voltage and current. The three phase unbalance is calculated by applying (3.16) to the current and voltage measurement.

$$\%V_{unbalance} = 100 \times \frac{V_{negative\ sequence}}{V_{positive\ sequence}} \tag{3.16}$$

The weekday voltage and current unbalance in Figure 3.27 and Figure 3.28 are calculated on the transformer LV terminal of the three grids considered:

- A small 24 unit complex connecting to the MV grid via a 100 kVA transformer
- A medium sized 45 unit complex connected to a 200 kVA transformer
- A larger sized 81 unit complex connected to a 315 kVA transformer

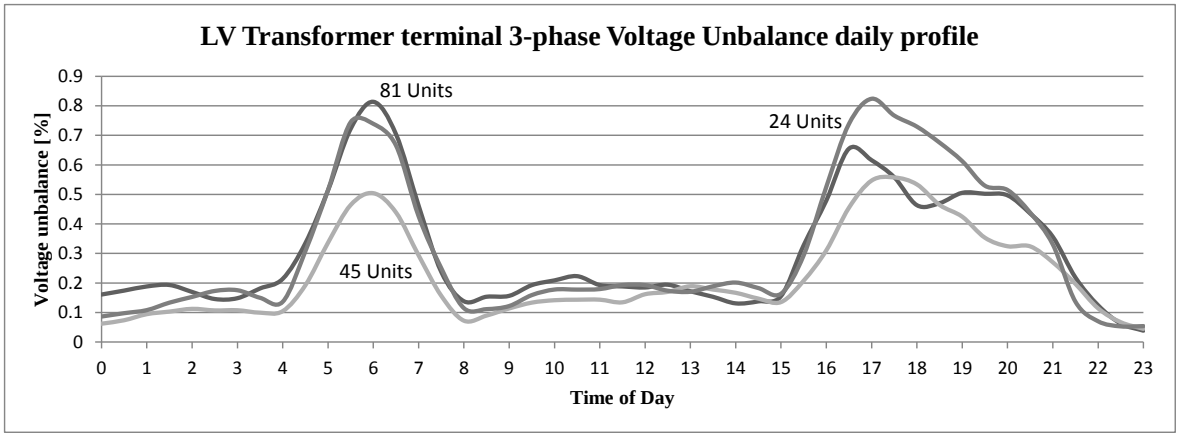

Figure 3.27. Daily voltage unbalance profile measured at LV transformer terminal.

The voltage unbalance is not expected to exceed 0.9% during the daily demand profile as seen in Figure 3.27. The maximum voltage unbalance of the 81 unit complex and the 24 unit complex are very similar in size, but the voltage unbalance of the 45 unit complex is 70% of the other sizes. The reason for this discrepancy is that the ratio between the diversified demand and the transformer rating of the 45 unit complex is 90%, while the

ratio between the loading and the transformer rating in the other two cases is close to 100%. The same trend is observed in the current unbalance in Figure 3.28.

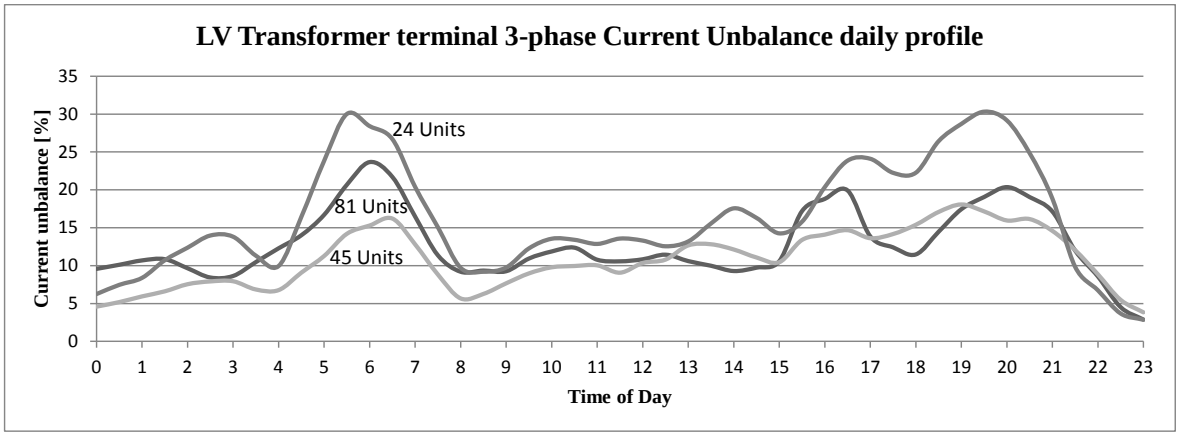

Figure 3.28. Daily voltage unbalance profile measured at LV transformer terminal.

The current unbalance in Figure 3.28 can exceed 30% for smaller complexes during times of peak demand. The profile of the current unbalance is a function of the loading of the grid. During times of high demand, the voltage and current unbalance are larger than during times of low demand. The current unbalance causes currents to circulate in the transformer delta winding. The delta winding of the MV transformer is rated for a line-line voltage of 11 kV.

In the simulation study of the sample 45 unit complex with integrated embedded generation, the unbalance simulation network is the same as the voltage regulation network. The simulation parameters and the operating scenarios are also the same. However, all PV systems are connected to Phase-A to simulate the largest possible unbalance. As there is no regulating body ensuring that all the PV systems are installed to minimize current and voltage unbalance, it is probable that some level of unbalance will prevail. The simulation result will be the maximum possible unbalance resulting from the embedded generation. To isolate the effect of the embedded generation, the load is perfectly balanced and all residential units are represented by identical loads. This assumption is based on the nature of PV systems which generate the maximum power during the time of the lowest demand and lowest load unbalance during the day.

3.4.3 Harmonic Emissions simulation method

The harmonic emission resulting from the grid connected inverters are simulated by injecting the maximum harmonic currents in Table 3.7 which were determined from the simulation of the inverter connected to the grid under changing output power and irradiation level. The angles of the current harmonics change very sporadically as they are functions of grid voltage magnitude and phase, grid frequency as well as inverter DC voltage, controller parameters, switching frequency and output current. For this reason the harmonics injected at all the residential connection points in the simulation model are based on a frequency sweep with varying phase angle between 0° and 360° for each of the harmonics up to the 31st. The magnitudes of the load and inverter harmonic currents injected are presented in Table 3.7. The resulting harmonic voltages and currents calculated on the transformer LV terminals represent the diversified emissions of different penetration levels of embedded PV generators. The harmonic currents are expressed in percentages based on the 200 kVA transformer ratings. The voltages are expressed as percentages of the rated fundamental frequency grid voltage.

The simulation is conducted under minimum load and minimum short circuit levels as the resistive and inductive damping is less under these conditions, resulting in the highest harmonic currents and voltages appearing on the transformer LV terminal. The harmonic currents in Table 3.7 are the maximum currents that occur for different levels of irradiation and power set-point. It is not necessarily possible that all the maximum magnitudes of the individual harmonic currents coincide. The randomly varying phase angles will reduce the error of this assumption due to the diversification. The harmonic current magnitudes in Table 3.7 show that the load currents above the 7th harmonic are similar in magnitude to the inverter emissions despite drawing a fundamental current 10 times smaller

Table 3.7 Harmonic current injection magnitude.

	Electronic load harmonic current		PV inverter harmonic current	
Harm #	% Fund	I_h [A]	% Fund	Ih [A]
1	100	1.7	100	17.3
3	60.6	1.03	45.68	7.90
5	56.5	0.96	9.64	1.67
7	50.6	0.86	6.06	1.05
9	44.7	0.76	4.75	0.82
11	38.2	0.65	4.68	0.81
13	30.6	0.52	1.89	0.33
15	24.1	0.41	1.55	0.27
17	18.2	0.31	0.94	0.16
19	12.9	0.22	0.76	0.13
21	8.8	0.15	0.76	0.13
23	5.9	0.1	0.77	0.13
25	4.7	0.08	0.57	0.10
27	4.1	0.07	0.27	0.05
29	4.1	0.07	0.22	0.04
31	3.5	0.06	0.20	0.04

CHAPTER 4 RESULTS

4.1 SIMULATION RESULTS

The purpose of the simulations is to identify power quality problems that pose a challenge as the penetration level of embedded PV generation in a high density residential cluster increases. The simulated results are compared to the quantified criteria from the power quality standards and design and planning guidelines of distribution grids. The simulation model consists of a 45 unit residential complex. The ratio between transformer impedance and loading is relatively linear, which means that the results from the simulation are applicable to different complex sizes. The loading is based on the diversified maximum demand which remains fairly constant for complexes where more than 20 units connect to a shared feeder.

4.1.1 Voltage Regulation

Voltage regulation is compared to the NRS 097-2-3 criteria stating that the combined embedded generation sharing a single feeder does not increase the voltage at the PCC by more than 3% when in service. In the simulation model, the point of connection is the LV terminal of the distribution transformer. The simulation network is compiled with the PV generators in service, each injecting 4 kW into the distribution grid. The voltage regulation is measured by disconnecting all the embedded PV generation, while recording the transformer LV winding positive sequence voltage.

Case 1: 10% embedded generation penetration level

Case 2: 25% embedded generation penetration level

Case 3: 40% embedded generation penetration level

The voltage regulation determined at the transformer LV windings for Case 1, Case 2 and Case 3 are summarized in Table 4.1. The voltage variation is simulated for a peak and minimum load case as well as under a high and a low short circuit level.

Table 4.1 Voltage regulation due to Embedded Generation.

Case	Load = 90% SCL = 3.7 MVA	Load = 45% SCL = 3.7 MVA	Load = 90% SCL = 3.2 MVA	Load = 45% SCL = 3.2 MVA
1	$\Delta V_{Trf,LV}$ = 0.26% ΔV_{Load} = 0.43%	$\Delta V_{Trf,LV}$ = 0.17% ΔV_{Load} = 0.46%	$\Delta V_{Trf,LV}$ = 0.56% ΔV_{Load} = 0.13%	$\Delta V_{Trf,LV}$ = 0.17% ΔV_{Load} = 0.77%
2	$\Delta V_{Trf,LV}$ = 0.87% ΔV_{Load} = 0.62%	$\Delta V_{Trf,LV}$ = 0.56% ΔV_{Load} = 0.75%	$\Delta V_{Trf,LV}$ = 0.95% ΔV_{Load} = 0.95%	$\Delta V_{Trf,LV}$ = 0.26% ΔV_{Load} = 0.39%
3	$\Delta V_{Trf,LV}$ = 1.04% ΔV_{Load} = 1.14%	$\Delta V_{Trf,LV}$ = 0.97% ΔV_{Load} = 1.05%	$\Delta V_{Trf,LV}$ = 1.96% ΔV_{Load} = 1.80%	$\Delta V_{Trf,LV}$ = 0.38% ΔV_{Load} = 0.41%

The voltage variation results from the reduction in load current through the cable sections. Reducing the current results a smaller voltage drop, resulting in a higher PCC voltage. The change in total active power due to the disconnection of the PV generators is 20 kW, 48 kW and 80 kW for Case 1, Case and Case 3 respectively. The largest change in voltage calculated on the transformer LV windings is 0.95% for the maximum stipulated penetration level of 25%. When the penetration is increased to 40%, the transformer LV voltage can change by almost 2% when all embedded generation is disconnected simultaneously. The voltage change measured on the load side of the longest cable is 1% when the penetration level is 25%. As the loads are modelled by a constant impedance, the active power loading reduces by the voltage squared, resulting in a smaller load side voltage variation.

From these results and Figure 3.24 it is clear that the short circuit level has a significant impact on the voltage variation.

4.1.2 Unbalance

The unbalance is calculated from the simulation model with increasing penetration level of PV systems, connected to the same phase. For this calculation the residential appliance load is balanced across the three phases. The unbalance is calculated under different loading levels and short circuit scenarios. The cases considered are:

Case 1: 10% embedded generation penetration level

Case 2: 25% embedded generation penetration level

Case 3: 33% embedded generation penetration level

The planning level for voltage unbalance in LV networks is 1.5%. The compatibility limit for unbalance is 3%. The voltage unbalance values in Table 4.2 are compared to the compatibility limit. The standards and planning guidelines are silent on the current unbalance. The current unbalance is however measured in the simulation to evaluate the relationship between voltage and current unbalance.

Table 4.2 Unbalance on Transformer LV winding.

Case	Load = 90% SCL = 3.7 MVA	Load = 45% SCL = 3.7 MVA	Load = 90% SCL = 3.2 MVA	Load = 45% SCL = 3.2 MVA
1	$V_{unbalance}$ = 0.5% $I_{unbalance}$ = 10.6%	$V_{unbalance}$ = 0.6% $I_{unbalance}$ = 29.6%	$V_{unbalance}$ = 1.1% $I_{unbalance}$ = 18.4%	$V_{unbalance}$ = 0.7% $I_{unbalance}$ = 26.3%
2	$V_{unbalance}$ = 2.0% $I_{unbalance}$ = 42.2%	$V_{unbalance}$ = 2.0% $I_{unbalance}$ = 81.6%	$V_{unbalance}$ = 2.0% $I_{unbalance}$ = 35.2%	$V_{unbalance}$ = 1.8% $I_{unbalance}$ = 77.2%
3	$V_{unbalance}$ = 2.3% $I_{unbalance}$ = 49.9%	$V_{unbalance}$ = 2.4% $I_{unbalance}$ = 91.4%	$V_{unbalance}$ = 3.1% $I_{unbalance}$ = 79.8%	$V_{unbalance}$ = 3.1% $I_{unbalance}$ = 79.8%

The simulation results indicate that the voltage unbalance planning limit of 1.5% is exceeded when the EG penetration level exceeds 25%. The voltage unbalance compatibility limit of 3% is only exceeded if the penetration level reaches 33% and the short circuit level is 3.2 MVA.

The current and voltage unbalance do not have a strong correlation. The current unbalance is strongly influenced by the short circuit level in the 11 kV grid, while the voltage

unbalance is more a function of the loading. Both, voltage- and current unbalance increase under increasing penetration levels of embedded generation, when all generators are connected to the same phase.

4.1.3 Harmonic Voltage and Current Emissions

The focus of this study is to assess the change in harmonic voltage and current profile measured at the LV terminal of the distribution transformer when embedded generation is connected at the load terminals in the simulation model. The study assesses the harmonic profiles of the 400 V grid under increasing penetration levels of inverter PV systems.

Harmonic impedance calculation

The harmonic impedance is calculated on the LV transformer terminals. The impedance results are used to identify frequencies where harmonic currents or harmonic voltages may be magnified by parallel and series resonance points. For each of the following cases, the positive sequence harmonic impedance is calculated on the distribution transformer LV terminal.

Base Case: No generation; Short Circuit Level (SCL) = 3.7MVA vs SCL = 3.2MVA

Case 1: 10% embedded generation penetration level

Case 2: 25% embedded generation penetration level

Case 3: 40% embedded generation penetration level

The impedances for each of the cases are calculated for a minimum load scenario with 2 kVA loads. Figure 4.1 investigates the effect of the 11 kV short circuit level on the harmonic impedance on the 400V terminal of the transformer. Case 1, Case 2 and Case 3 investigate the effect of the PV system L-C filters on the harmonic impedance for different penetration levels. The L-C filters are represented by the filter capacitance of 5µF.

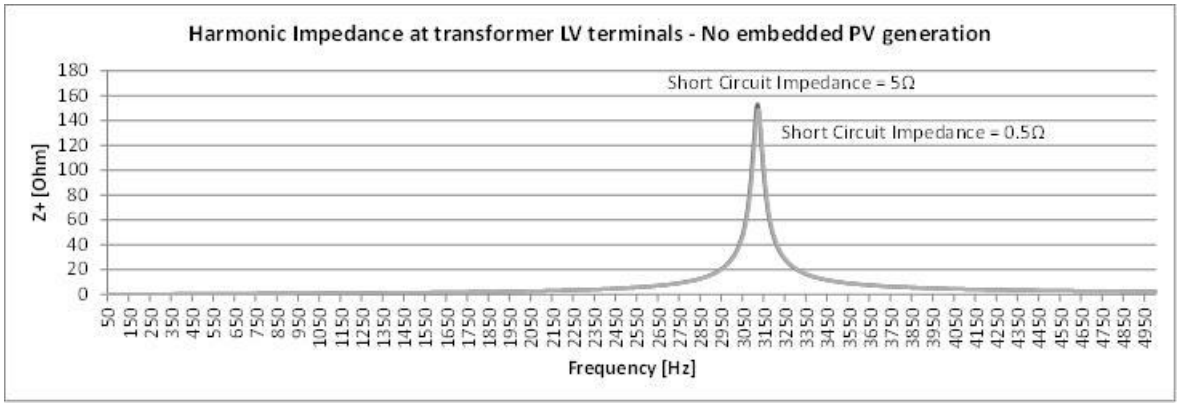

Figure 4.1. Harmonic impedance of grid calculated on transformer LV terminal.

From Figure 4.1 it can be seen that change in harmonic impedance due to changes in short circuit level is very small, indicating that the transformer impedance isolates the 400 V grid from the 11 kV network.

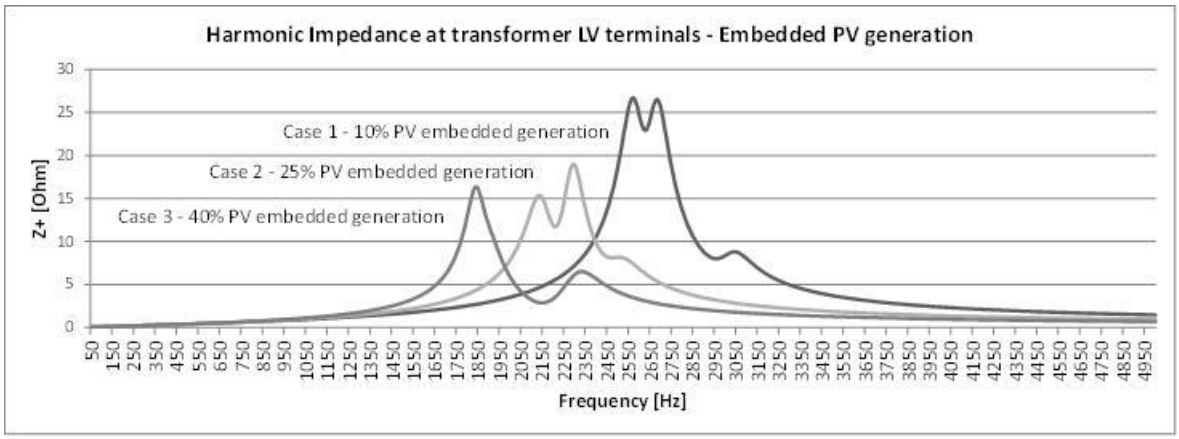

Figure 4.2 Harmonic impedance of grid with EG calculated on transformer LV terminal.

Figure 4.2 indicates the effect of the inverter L-C filters on the harmonic impedance measured on the transformer LV terminals. The parallel resonance occurs anywhere between 1.8 kHz and 2.8 kHz, depending on the penetration level. With a higher penetration level the parallel resonance point shifts towards the lower frequencies as a function of the combined capacitance and the cable inductance.

Harmonic current injection

The directly connected induction machines and thermal loads such as space heaters, geysers and kettles introduce very little harmonic content into the grid. Electronic loads such as CFLs, TVs and computers amongst others are power by rectified DC current. The square current waveform creates high odd harmonic currents due to the full-wave rectifiers employed. For this study, the harmonic currents of the three most significant loads are added by Root Sum Squared (RSS) resulting in the currents in Table 3.7 for a combined 400 W load. These harmonic currents are then injected where the domestic loads connect in the simulation grid at randomly rotating phase angles resulting in diversified harmonic current and voltage profile on the transformer LV terminal as seen in Figure 4.3 and Figure 4.4.

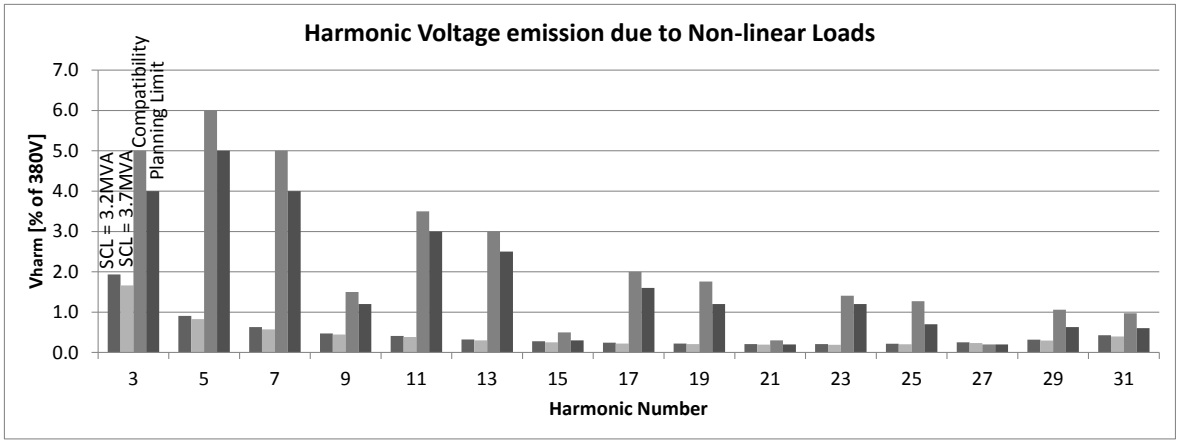

Figure 4.3. Harmonic Voltage profile at LV transformer terminal – Load harmonic emissions.

A 15% reduction in short circuit level increases the 3rd harmonic voltage by 15%. The magnification of the higher frequency harmonic voltages reduces to 7% by the 31st harmonic. The harmonic voltage planning limit is exceeded for the odd harmonic numbers which are multiples of 3 for harmonics greater than the 21st harmonic. The 27th harmonic compatibility limit is also exceeded.

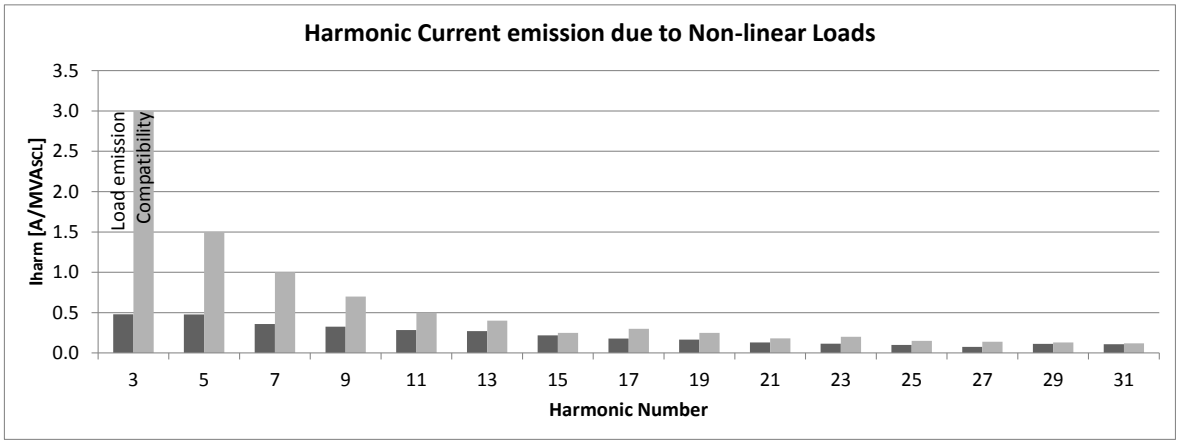

Figure 4.4. Harmonic Current profile at LV transformer terminal – Load harmonic emissions.

The harmonic currents emitted by the electronic loads are below the NRS 097 compatibility limits. At the higher frequencies the margin between the limit and the emissions becomes very small.

For the assessment of the harmonics due to the PV systems distributed throughout the grid, the harmonic emissions of the loads have been omitted. The background harmonics in the rest of the MV grid have also not been accounted for. The three penetration levels investigated in the study are:

Case 1: Embedded generation is 10% of transformer rating

Case 2: Embedded generation is 25% of transformer rating

Case 3: Embedded generation is 40% of transformer rating

For each of the cases the magnitudes of harmonic current and voltage are calculated. The cases are calculated under peak and minimum load scenario and for a short circuit level of 3.7 MVA and 3.2 MVA. The magnitudes of the odd harmonics in Figure 4.5 and Figure 4.6 are the maximum values of the four load and short circuit scenarios considered.

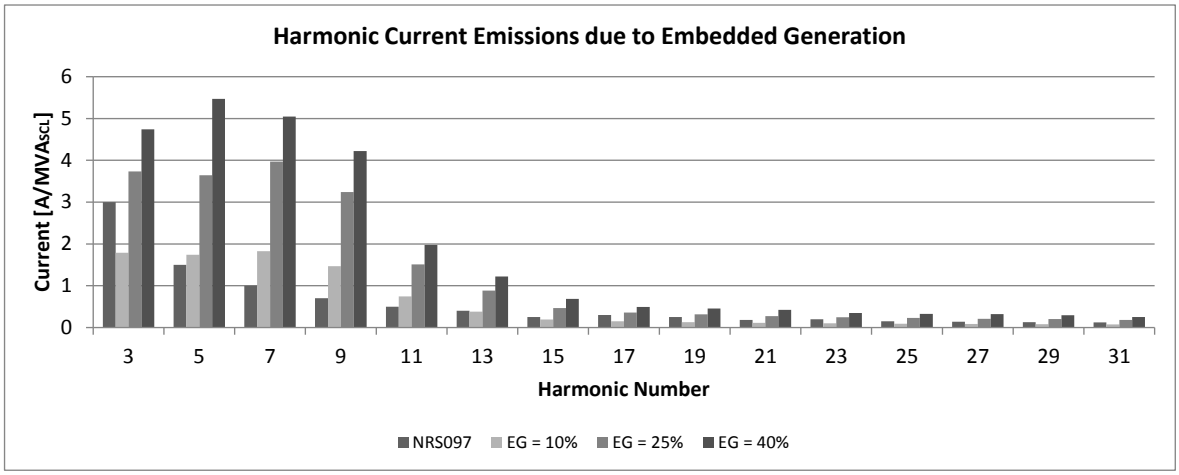

Figure 4.5. Current harmonic emissions calculated on the transformer LV terminal.

The harmonic current limits contained in the NRS 097 planning guide are exceeded for penetration levels of 25%. It should be noted that the simulated magnitudes correspond to the maximum harmonics that are generated during low irradiation levels. The emissions of the various harmonics depicted in Figure 4.5 might not all occur simultaneously as the peak harmonic currents are dependent on the power output or irradiation level as shown in Figure 3.21.

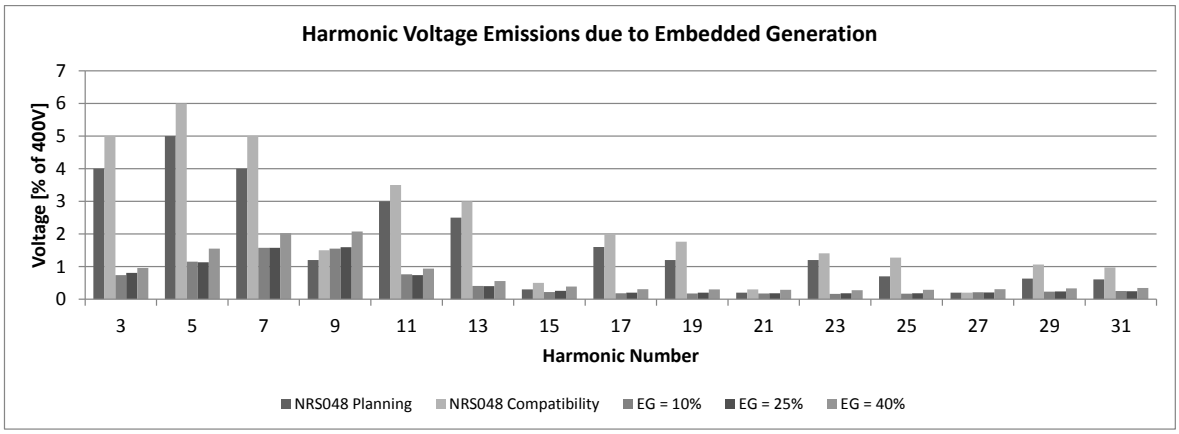

Figure 4.6. Voltage harmonic emissions calculated on the transformer LV terminal.

The harmonic voltage planning and compatibility limits are only exceeded for the odd harmonics that are multiples of three. Due to the unbalance in the distribution grid, there is a zero-sequence path for the triplen harmonics to enter the transformer delta winding resulting in larger harmonic voltages than the standards anticipate in a balanced network.

The calculated Total Harmonic Distortion is 3.4% for a penetration level of 25% and 4.2% when the penetration level reaches 40%.

4.2 SUMMARY

The hypothesis is tested by comparing the planning and compatibility levels of the power quality standards and the planning guidelines with simulation results of possible distribution grid scenarios determine if the standards and guidelines need to be amended to address power quality challenges that may arise due to increasing penetration levels of embedded PV generation in high density residential cluster distribution grids.

The simulation model that was used to calculate the expected voltage variation, unbalance and harmonic emissions due to grid connected PV inverters is based on the planning criteria stating maximum penetration level, maximum generation capacity of individual generators, short circuit levels, cable lengths and loading. The load model suggested in the guidelines was found to be 20% larger than what field measurements showed. The load model used in the simulation is based on the measurement data and scaled to give a peak load of 4.0 kVA with a power factor of 0.9 as well as a minimum load of 2.0 kVA with a power factor of 0.9. The NRS 097 planning guideline suggests that the penetration level of embedded generation connected to a shared feeder should not exceed 25%. Table 4.3 summarises the simulation results and compares these to the respective planning criteria.

Table 4.3 Summary of simulation results – PV penetration level = 25%.

	Planning Level	Compatibility Level	Simulation Result
Voltage regulation	3.0%	+/-15%	0.95%
Voltage unbalance	2.0%	3.0%	2.0%
Voltage THD	5%	8%	3.4%
Current Unbalance	Not mentioned	Not mentioned	82%
Current THD	5%	Not mentioned	7.5%

For a penetration level of 25% of embedded generation in a high density residential complex, the voltage quality limits stated in the power quality standards listed in Table 4.3 are not exceeded. The current limits are not well defined. The NRS 097 standard stipulates

a maximum current THD of 5% of the rated fundamental current of a new device connecting to the grid. The current THD is exceeded for an embedded generation penetration level of 25%. The standards and guidelines remain silent on current unbalance limits. The unbalance simulation considered all PV generators connected to the same phase, which is very unlikely. The maximum simulated current unbalance is then 82%. Without the PV generation embedded in the distribution grid, the unbalance in the LV network may reach levels of 35% for short periods during any given day.

The harmonic voltages and currents for the odd harmonics are presented in Table 4.4 and Table 4.5 respectively. The voltage harmonics limits are well defined in the NRS 048 quality standards, providing planning and compatibility limits. The IEEE and IEC have different methods of referencing the harmonic currents. The IEEE bases the current harmonics on the equipment rating of the fundamental frequency current, while the IEC standardizes the individual harmonics based on the short circuit level. The harmonic current simulation results and the NRS 048 limits are both referred to a short circuit level of 3.7 MVA on the transformer LV winding in Table 4.5.

Table 4.4 Odd Harmonic voltage emission summary – LV transformer terminal.

Harm #	Planning	Compatibility	EG = 10%	EG = 25%	EG = 40%
3	4.00	5.00	0.74	0.81	0.96
5	5.00	6.00	1.15	1.13	1.55
7	4.00	5.00	1.57	1.58	2.02
9	1.20	1.50	1.55	1.60	2.08
11	3.00	3.50	0.76	0.74	0.94
13	2.50	3.00	0.41	0.40	0.56
15	0.30	0.50	0.22	0.26	0.39
17	1.60	2.00	0.18	0.20	0.30
19	1.20	1.76	0.17	0.20	0.30
21	0.20	0.30	0.17	0.18	0.29
23	1.20	1.41	0.17	0.18	0.28
25	0.70	1.27	0.17	0.18	0.29
27	0.20	0.20	0.21	0.21	0.30
29	0.63	1.06	0.23	0.24	0.33
31	0.60	0.97	0.25	0.24	0.34
33	0.20	0.20	0.27	0.28	0.39
35	0.56	0.83	0.28	0.28	0.40
37	0.54	0.77	0.20	0.21	0.34
39	0.20	0.20	0.19	0.23	0.37

The 9^{th}, 27^{th} and 33^{rd} harmonic voltage planning and compatibility limits from the NRS 048 standard are exceeded regardless of the Embedded Generation (EG) penetration level as seen in Table 4.4. The other odd harmonic voltages are not exceeded. The voltage quality criteria are generally not exceeded in LV distribution networks as the transformer impedance isolates the LV grid to a certain extent from the MV grid. The triplen harmonic limits are very low as these are expected to cancel in the transformer delta winding of a

balanced three-phase system. Due to the many single-phase loads and generators, the unbalance between the phases permits the triplen harmonic currents to circulate in the transformer delta windings giving rise to larger triplen harmonic voltages than the respective limits.

The current harmonic emissions and the respective limits in Table 4.5 are given in A/MVA_{SCL}, where a short circuit level of 3.7 MVA.

Table 4.5 Odd harmonic current emissions summary – LV transformer terminal.

Harmonic	NRS097	NRS048	EG = 10%	EG = 25%	EG = 40%
3	3.00	3.12	1.79	3.73	4.74
5	1.50	3.12	1.74	3.64	5.47
7	1.00	3.12	1.83	3.97	5.05
9	0.70	3.12	1.47	3.24	4.22
11	0.50	1.56	0.74	1.51	1.98
13	0.40	1.56	0.38	0.88	1.22
15	0.25	1.56	0.19	0.47	0.68
17	0.30	1.17	0.15	0.36	0.49
19	0.25	1.17	0.13	0.32	0.46
21	0.18	1.17	0.11	0.27	0.42
23	0.20	0.47	0.10	0.25	0.35
25	0.15	0.47	0.09	0.23	0.33
27	0.14	0.47	0.09	0.21	0.32
29	0.13	0.47	0.08	0.20	0.29
31	0.12	0.47	0.08	0.18	0.25
33	0.11	0.47	0.07	0.18	0.27
35	0.11	0.23	0.07	0.17	0.24
37	0.10	0.23	0.07	0.17	0.25
39	0.10	0.23	0.07	0.16	0.25

Most of the harmonic current limits in Table 4.5 are exceeded regardless of the embedded generation penetration level.

The simulation results are compared to the power quality limits to test the hypothesis in qualitative terms. The voltage limits are not exceeded when the penetration level of embedded generation is 25%. The definition and the limits of the power quality aspects relating to currents are not well defined in the standards and guidelines. It is very difficult to define the limits given that the power ratings and the short circuit levels are grid specific and can vary according to the operation mandate of a distribution network. Excessive current unbalance in combination with high harmonic emissions resulting from the grid connected PV inverters will have an effect on the equipment life cycles if the equipment is not rated accordingly. The planning guidelines do not address the subject of current quality sufficiently to allow a standard approach to be followed once embedded generation penetration levels reach the proposed 25% level. When the embedded generation penetration level exceeds 25% some of the voltage compatibility limits are also exceeded.

CHAPTER 5 DISCUSSION

The failure of several collection grid transformers in two of the recently commissioned commercial PV plants in de Aar, South Africa was attributed to high frequency currents injected into the transformer LV terminals causing significant voltages to appear between the windings and ground due to stray capacitances. The failure phenomenon is also described in [55]. Excessive gassing caused the Buchholz relays to operate taking several transformers out of service. There are parallels that can be drawn between these commercial PV plants and high density residential clusters with high penetration levels of small scale embedded PV generation:

- Both employ similar distribution type transformers to connect to an MV grid
- Both employ grid connected inverters connected to the transformer LV winding
- Both are connected to grids with high levels of background harmonics

These parallels are the motivation for this research and prompt the hypothesis that the integration of embedded generation in high density residential housing distribution systems requires technical design and planning criteria to be reviewed and amended where necessary.

The planning and design criteria assume that the power quality in distribution grids is within limits defined in the NRS 048 power quality standards. With the many technological advances made in recent years the residential load profile has changed from mostly passive loads to a mix of electronic and passive loads, as well as the widespread integration of inverter based embedded generation. On distribution level, there is a lack of accountability as it is practically not possible to assign responsibility to individual residential customers. It is therefore the responsibility of the distribution grid design and planning department of the municipalities and utilities to rate and size the distribution equipment with sufficient margin to ensure that the life cycle expectations of the

equipment are met. The guidelines have to be reviewed to ensure that the planning and compatibility levels, forming the basis of the equipment specifications, accommodate the additional stresses associated with high penetration levels of small scale embedded PV generation. The South African standard for power quality NRS 048 references the IEC 61000-3-6 and IEEE-519 documents regarding the apportionment method of new connections [4]. The planning guidelines should state whom responsibility is assigned to for complying with the power quality limits when multiple residences connect to a shared feeder.

5.1 VOLTAGE REGULATION

The voltage variation should not exceed 3% when all embedded generation is connected or disconnected simultaneously as described in the NRS 097 planning guidelines. It is very unlikely that all generators connect simultaneously and inject the maximum power into the grid instantaneously. Typical generators ramp the output power over a couple of seconds as defined by the controller time constant and gain. It is also unlikely that all devices switch off simultaneously. In practice, such a scenario could only be observed when the network frequency changes in excess of the inverter design limit, without affecting the voltage of the distribution grid. The magnitude of the voltage variation resulting from the disconnection of the embedded generation depends on the network loading, the system short circuit level and on the penetration level of embedded generation. The magnitude of the resulting voltage variation increases with increasing penetration level. The short circuit level also affects the magnitude of the variation as the voltage variation can be approximated by dividing the change in reactive power by the short circuit level. A lower short circuit level therefore results in a larger voltage variation. The distribution transformer impedance has the greatest effect on the short circuit level in the LV grid. Transformers with higher ratings allow higher short circuit currents, resulting in lower voltage variations. It is therefore expected that larger complexes with larger transformers would be subjected to smaller voltage variations, while smaller complexes would experience relatively larger variations.

From the simulation results it can be deduced that a voltage variation in excess of the 3% planning limit is highly unlikely as the PV generator systems considered in this research

are not able to absorb or inject any reactive power in accordance with NRS 097. Compared to the short circuit level, the change in reactive power absorbed by the cables due to changing load current is very small resulting in a maximum voltage variation of +/-1% for a 25% penetration level. The voltage variation experienced by other customers is also less than 1%. As embedded generation penetration levels approach 40% the voltage variation due to the disconnection of all PV generators can exceed 2% when the grid is heavily loaded and the short circuit level is relatively low.

Using the trend identified in Figure 3.26, relating the voltage variation to the transformer rating, it can be deduced that smaller complexes with 20 units can experience a voltage variation on the LV side that is up to 10% greater than that of the 45 unit grid when the 25% embedded generation is disconnected.

5.2 UNBALANCE

The voltage unbalance planning limit of 1.5% is not exceeded when the penetration level is 25% and all embedded generation is connected to the same phase. During the time when the solar irradiation is at its highest and the largest unbalance due to the embedded generation can be expected, the unbalance of the load is at its lowest. The compliance limit of 3% is exceeded if the penetration level approaches 33% and all the embedded generation is connected to the same phase. In practice it is unlikely that all generation is connected to the same phase. As stated in the NRS 097 planning guideline, care should be taken that the generators assist in the three phase balancing.

The current unbalance is 82% when the penetration level is 25% and all embedded generation is connected to the same phase. The current unbalance is much higher than the voltage unbalance due to the grounded wye transformer winding. The unbalance on the MV grid is about 5 times smaller than the unbalance the LV grid as the delta-wye transformer has a high negative phase sequence reactance preventing the unbalance to mitigate to the MV grid. The current unbalance is also influenced by the short circuit level and the loading of the network. A current unbalance creates a path for zero-sequence harmonics, like the 3^{rd}, 9^{th} and 15^{th} harmonic to pass through the transformer delta windings and enter the 11 kV grid. A high current unbalance increases the transformer

losses and temperature [54] and has to be addressed in the design of the transformer by adding margin to the current ratings.

5.3 HARMONIC EMISSIONS

The voltage harmonics are defined as percentages of the voltage rating and are therefore well defined. The current harmonics are a bit more difficult to per unitise as various equipment and grids have a different current ratings. The IEEE uses the short circuit level at the point of connection as the reference while the IEC uses the current rating of the respective system. Both of these approaches are very subjective as they do not give a concise representation of the magnitude of the harmonic currents at all times as ratings and short circuit level can change depending on equipment outages and operating mandates. Harmonic currents cause losses and temperature rises in distribution equipment, be it transformers or cables [53]. The loss of life calculation can be used to estimate the effect of harmonic currents on the life cycle of transformer isolation material.

The harmonic currents emitted by the embedded generation vary according to the output of the inverters. The harmonic currents were shown to be at their highest during the twilight hours of the day when the irradiation is below 400W/m^2. Although the high harmonic currents coincide with increased loading, the overlapping period of the high load current and the high harmonic currents is very short. The temperature rise coefficient is slow enough that it is not expected that equipment life cycles will be impacted significantly.

From a regulatory perspective, the peak harmonic currents due to penetration levels of 25% regularly exceed the limits defined in the NRS 097 standards. The available harmonic voltage margin between the existing background harmonics and the planning limits has to be calculated to assess the apportionment limits that apply to new grid connections. The point of connection of the high density residential cluster is the LV terminal on distribution transformers. The NRS 097 standard requires that the harmonic voltage distortion limits applicable to Stage 1 devices are adhered to. Since the integration of individual PV systems into the low voltage distribution grid is expected to transpire over a long time, the apportionment methods proposed by the IEEE and the IEC have several short-comings. The apportionment limits for future grid connection applications would become very onerous as the background harmonics from the inverters occupy increasing margins as

more devices are integrated. Assigning a 1% voltage apportionment limit to the total harmonic voltage distortion, as proposed in the NRS 097 guideline for Stage 1 devices is also not viable as the total harmonic distortion of all inverters together would surpass the compliance levels of 5% measured at the common supply point.

Most of the even voltage harmonics exceed the limits, even for penetration levels below 25%. The voltage limits of the even harmonics are very onerous for a reason; High DC content can cause transformers to saturate. When transformers saturate the losses and operating temperature increases the transformers start contributing to the harmonic distortion by clipping the voltage sinusoid [53].

The findings presented in this dissertation are based on a 45 Unit residential complex. Smaller complex LV grids with 20 units are connected to the MV grid with smaller rated transformers having a higher loading to short circuit level than larger complexes. From the calculations and simulations performed in Chapter 3, it can be deduced that the voltage variation, voltage unbalance and voltage harmonic emissions will be up to 10% greater for a 20 unit complex than those calculated for the 45 unit complex. The voltage quality of complexes larger than the 45 unit complex is expected to be marginally better.

CHAPTER 6 CONCLUSION

The research gap that was identified pertains to power quality challenges that arise due to high penetration levels of small scale embedded PV generation in South African high density residential clusters. The research questions ask whether existing distribution equipment can accommodate the additional power quality stresses due to the grid connected PV inverters and how the distribution equipment life cycles are affected. The hypothesis developed in response to these questions is that the existing planning and design standards and guidelines have to be revised to ensure that future grids are designed according to a radically changing residential load profile.

The research follows an engineering-orientated approach combining quantitative and qualitative methods to test the hypothesis:

- The hypothesis is first translated to quantifiable power quality criteria that can be tested in a simulation model.
- The simulation model is then developed based on existing research and practical experience. The load model, which is compiled to represent South African households in high density clusters, is verified against field measurements.
- The simulation model is used to investigate the impact of different penetration levels of embedded generation on voltage regulation, unbalance and harmonic emissions.
- The simulation results are compared to the power quality criteria to arrive at the conclusion that certain elements of the planning standards have to be revised to accommodate practical penetration levels of small scale embedded PV generation.

The correlation between increases in embedded generation penetration levels and voltage variation, unbalance and harmonic emissions are determined by simulating various operating scenarios of varying load and short circuit level for penetration levels of 10%,

25% and 40%. The existing distribution grid planning guideline limits the penetration level of embedded generation to 25% of the rating of the shared distribution transformer.

Some of the limits contained in the South African power quality standards NRS 048 and the distribution grid planning guidelines NRS 097 are exceeded when penetration levels of grid connected PV generation approach 25%.

- Switching embedded generation in or out of service does not cause voltage variations that exceed the planning limit of 3%.
- Voltage unbalance due to embedded generation connected to the same phase does not cause the compatibility limit of 3% to be exceeded.
- Current unbalance should be monitored as it is very likely that equipment ratings may be exceeded when the integration of embedded generation is not coordinated and balanced.
- Only voltage limits of the odd harmonics which are multiples of 3 are exceeded.
- Current harmonic planning limits of several harmonics are exceeded, even for penetration levels less than 25%.

There are three approaches that can be followed to mitigate the challenges associated with the power quality aspects addressed in this research:

1. Restrict the penetration levels of embedded generation even further
2. Assign authority to ensure that load and generation is balanced across the phases.
3. Install active filters to attenuate harmonic currents and voltages
4. Add more margin to the current and voltage ratings of distribution equipment

The hypothesis has been tested in qualitative terms and found to test true. Power quality aspects relating to current unbalance and harmonic currents have to be addressed in the standards to avoid scenarios where future distribution grids and equipment are not rated to withstand the currents that are due to increasing penetration levels of embedded generation.

FUTURE WORK

It will be beneficial to the distribution network planning departments of utilities and municipalities, the equipment manufacturers and consumers if the theory contained in this work can be validated against power quality recordings of a high density residential cluster

once the penetration level of grid connected PV systems reaches the 25% level proposed in the NRS 097 planning guideline.

Further research should be initiated into the control requirements of embedded generation that can be translated to a set of standards that mitigate stability challenges and increase system security.

REFERENCES

[1] V.U. Hoffmann, "Damals war's: Ein Rückblick auf die Entwicklung der Photovoltaic in Deutschland", *Sonnenenergie*, pp. 38-39, Dec. 2008.

[2] Simplified utility connection criteria for low-voltage connected generators, NRS 097-2-3, 2014.

[3] R. du Plesis, R. Jansen van Rensburg, "The rise of Estate living", *Lightstone Property Newsletter*, Nov. 2013.

[4] Electricity Supply – Quality of Supply, NRS 048:2003, 2003.

[5] M. Yazdani-Asrami, M. Mirzaie, A. Akmal, "Investigation on Impact of Current Harmonic Contents on the Distribution Transformer Losses and Remaining Life", in *IEEE International Conference on Power and Energy*, Malaysia, pp. 689 – 694, Nov. 2010.

[6] A. Collins, G. Tsagarakis, A. Kiprakis, S. McLaughlin "Development of Low-Voltage Load Models for Residential Load Sector", *IEEE Transactions on Power Systems*, vol. 29, no. 5, pp. 2180 – 2188, Sep. 2014. DOI: 10.1109/TPWRS.2014.2301949.

[7] P. Chen, R. Salcedo, Q. Zhu, "Analysis of Voltage Profile Problems Due to the Penetration of Distributed Generation in Low-Voltage Secondary Distribution Networks", *IEEE Transactions on Power Delivery*, vol. 27, no. 4, pp. 2020 – 2028, Oct. 2012. DOI: 10.1109/TPWRD.2012.2209684.

[8] Electricity distribution – Guidelines for the provision of electricity distribution networks in residential areas - Part1: Planning and design of distribution networks, NRS 034-1:2007, 2007.

[9] Grid Connection Code for Renewable Power Plants (RPPs) connected to the Electricity Transmission System (TS) or the Distribution System (DS) in South Africa, NERSA, 2014.

[10] A. Niasar, Z. Zare, F. Far, "A Low-Cost P&O based Maximum Power Point Tracking, Combined with Two-Degree Sun Tracker", presented at *6th International Power Electronics Drive Systems and Technologies Conference*, 3-4 Feb. 2015, Theran.

[11] T. Niknam, A. Ranjbar, A. Shirani, "Impact of Distributed Generation on Volt/VAr Control in Distribution Networks", in *IEEE Bologna Power Tech Conference proceedings*, 23 – 26 Jun. 2003, Bologna, Italy. DOI: 10.1109/PTC.2003.1304390.

[12] P. Moses, M. Masoum, "Three-phase Asymmetric Transformer Aging Considering Voltage-Current Harmonic Interactions, Unbalance Nonlinear Loading, Magnetic Couplings, and Hysteresis", *IEEE Transactions of Energy Conversion*, vol. 27, no. 2, pp. 318 – 327, Jun. 2012. DOI: 10.1109/TEC.2011.2181949.

[13] IEEE Recommended Practice and Requirements for Harmonic Control in Electric Power Systems, IEEE 519, 2014.

[14] H.W. Dommel, A. Yan, S. Wei, "Harmonics from Transformer Saturation", *IEEE Transactions on Power Systems*, vol. 1, no. 2, pp. 209 – 215, Apr. 1986. DOI: 10.1109/TPWRD.1986.4307952.

[15] S. Elphick, P Ciufo, S. Perera, "Laboratory investigation of the input current characteristics of modern domestic appliances for varying supply voltage conditions", in *Proceedings of 14th International Conference on Harmonics and Quality of Power*, pp. 1-7, 2010. DOI: 10.1109/ICHQP.2010.5625397.

[16] F. Barakou, M. Bollen, S. Mousavi-Gargari, O. Lennerhag, P. Wouters, E. Steennis, "Impact of Load Modeling on the Harmonic Impedance seen from the Transmission Network", in *Proceedings of 17th International Conference on Harmonics and Quality of Power*, pp. 283 – 288, 2016. DOI: 10.1109/ICHQP.2016.7783466.

[17] J. Schlabbach, "Harmonic Current Emission of Photovoltaic Installations under System Conditions", in *Proceedings of 2008 5th International Conference on the European Electricity Market*, pp. 1 – 5, 2008. DOI: 10.1109/EEM.2008.4579000.

[18] H. Mantilla, A. Pavas, I. Duran, "Aging of Distribution Transformers due to Voltage Harmonics", in *Proceedings of IEEE Workshop on Power Electronics and Power Quality Applications*, pp. 1 -5, 2017. DOI: 10.1109/PEPQA.2017.7981649.

[19] R. Kumar, "Assuring Transient Stability in the Smart Grid", in *IEEE PES Innovative Smart Grid Technologies*, pp. 1 – 6, 2012. DOI: 10.1109/ISGT.2012.6175778.

[20] Y. Xiaoling, W. Xuchang, H. Song, W. Bing, "Analysis on Interaction between Three Phase PV Grid-Connected Inverter and Weak Grid", in *Proceedings of 32nd Youth Academic Annual Conference of Chinese Association of Automation*, pp. 429 – 435, 2017. DOI: 10.1109/YAC.2017.7967447.

[21] B. Perera, S. Pulikanti, P Ciufo, S Perera, "Simulation Model of a Grid-Connected Single-Phase Photovoltaic System in PSCAD/EMTDC", in *Proceedings of IEEE International Conference on Power System Technology*, 2012. DOI: 10.1109/PowerCon.2012.6401435.

[22] B. Rao, N. Senroy, A. Abhyankar, "Analysis of OLTC behavior in a Wind Power Integrated Distribution System", in *Proceedings of the IEEE PES Asia-Pacific Power*

and Energy Engineering Conference, pp. 1-5, 7-10 Dec. 2014, Hong Kong. DOI: 10.1109/APPEEC.2014.7066133.

[23] Y. Wei Li, C. Kao, "An Accurate Power Control Strategy for Power-Electronics-Interfaced Distributed Generation Units Operating in a Low-Voltage Multibus Microgrid", *IEEE Transactions on Electronics*, vol. 24, no. 12, pp. 2977-2988, Aug. 2009. DOI: 10.1109/TPEL.2009.2022828.

[24] P. Irminger, D. Rizy, H. Li, T. Smith, F. Li, S. Adhikari, "Air conditioning stall phenomenon - Testing, model development, and simulation", in *IEEE Conference publication of PES T&D*, pp 1 – 8, 2012. DOI: 10.1109/TDC.2012.6281531.

[25] J. Wang, W. Pang, L. Wang, "Synthetic Evaluation of Steady-state Power Quality Based on Combination Weighting and Principal Component Projection Method", *CSEE Journal of Power and Energy Systems*, Vol. 3, No.2, pp. 160 – 166, Jun. 2017. DOI: 10.17775/CSEEJPES.2017.0020.

[26] A. Kannan, V. Kumar, T. Chandrasekar, B. Rabi, "A Review of Power Quality Standards, Electrical software tools, Issues and Solutions", in *Proceedings of International Conference on Renewable Energy and Sustainable Energy*, pp. 91 – 97, 2013. DOI: 10.1109/ICRESE.2013.6927794.

[27] CTLab, "ImpedoDuo, Power Quality Recorder User Guide", Feb. 2014. [Online]. Available: http://www.ctlab.com/downloads/Impedo_DUO_User_Guide.pdf

[28] T. Haggis, "e-on Central Networks: Network Design Manual Version7.7", Dec. 2006. [Online]. Available: https://www.pdffiller.com/en/project/129557865.htm

[29] South African Distribution Code: Network Code Version 6.0, NERSA, 2014.

[30] ActewAGL "Guidelines for embedded generator connection to ActewAGL low voltage (LV) network", March 2013. [Online]. Available: www.actewagl.com.au/

[31] W.L.O. Fritz and D.C. Kallis, "Domestic Load-profile Measurements and Analysis across a Disparate Consumer Base" presented at *Domestic Use of Energy Conference*, Cape Town, South Africa, Apr. 2009.

[32] Department of Energy, "A survey of energy-related behavior and perceptions in South Africa: The Residential Sector", 2012. [Online]. http://www.energy.gov.za/files/media/Pub/

[33] A.K. Hiranandani, "Effects of harmonics on the current carrying capacity of insulated power cables used in three phase electrical power distribution systems" in *Proceedings of 18th International Conference on Electricity Distribution*, pp 1 – 5, Jun. 2005. DOI: 10.1049/cp:20051044.

[34] M. Fahad, N. Arbab, "Factor Affecting Short Term Load Forecasting", *Journal of Clean Energy Technologies*, Vol. 2, No. 4, Oct. 2014.

[35] Y. Ramgolam, S. Veerapen, V. Oree, A. Murdan, K. Soyjaudah, "Energy Profiles and Performance of Common Electrical Domestic Appliances", in *Proceedings of IEEE International Energy Conference*, pp 1129 – 1136, May 2014. DOI: 10.1109/ENERGYCON.2014.6850565.

[36] G. Karaday, S. Saksena, "Effect of Voltage Sags on Loads in a Distribution System", Power Systems Engineering Research Centre, PSERC Publication 05-63, Oct. 2005. [Online]. Available: https://pserc.wisc.edu/documents/publications

[37] F. Quilumba, W. Lee, H, Huang, D. Wang, R. Szabados, "Load Model Development for Next Generation Appliances", in *Proceedings of IEEE Industry Applications Society Annual Meeting*, pp. 1 – 7, 2011. DOI: 10.1109/IAS.2011.6074402.

[38] D. Lv, J. Zhang, Y. Dai, "Study on time and frequency-domain harmonic models of single-phase full bridge rectifiers", presented at *5th Annual IEEE International Conference on Cyber Technology in Automation, Control and Intelligent Systems*, pp. 1186 – 1191, China, 8 - 12 Jun. 2015. DOI: 10.1109/CYBER.2015.7288112.

[39] Y. Begazi, M. Salama, "Calculations of Diversified Harmonic Currents in Multiple Converter Systems", presented at *Power Engineering Society Summer Meeting*, pp. 727 – 731, 2000. DOI: 10.1109/PESS.2000.867441.

[40] B. Enache, F. Birleanu, M. Radut, "Modeling a PV panel using the manufacturer data and a hybrid adaptive method", presented at *8th International Conference of Electronicsm Computers and Artificial Intelligence*, pp. 1 – 6, Jul. 2016. DOI: 10.1109/ECAI.2016.7861108.

[41] M. Liu, J. Huang, Y. Dong, H. Li, "Steady-state Control performance Modeling and Simulation Analysis for Grid-connected PV inverter", presented at *China International Conference on Electricity Distribution*, pp. 1 -4, 10-13 Aug. 2013. DOI: 10.1109/CICED.2016.7576195.

[42] J. Ishikawa, A. Nakata, A. Torii, K. Doki, S. Mototani, "A DC Voltage Estimation at the Maximum Power Point of a Series Parallel Connection PV System with Partial Shade", presented at *International Symposium on Micro-NanoMechatronics and Human Science*, pp. 1 – 6. 2014, DOI: 10.1109/MHS.2014.7006111.

[43] R. Yan, T. Kumar, "Investigation of Voltage Stability for Residential Customers Due to High Photovoltaic Penetrations", *IEEE Transactions on Power Systems*, vol. 27, no. 2, May 2012. DOI: 10.1109/TPWRS.2011.2180741.

[44] H.A. Mohamed, A. Khattab, A. Mobarka, G. Morsy, "Design, Control and Performance Analysis of DC-DC Boost Converter for Stand-Alone PV System", presented at *18th International Middle East Power Systems Conference*, pp. 101 – 106, 2016. DOI: 10.1109/MEPCON.2016.7836878.

[45] A. Latheef, V. Gosbell, V. Smith, "Harmonic Impact of Residential Type Photovoltaic Inverters on 11kV Distribution system", University of Wolong, Wollong, Australia,

2015. [Online]. Available: http://citeseerx.ist.psu.edu/viewdoc/

[46] J. Schlabbach, L. Kammer, "Prediction of harmonic currents of PV-inverters using measured solar radiation data", in *Proceedings of IEEE MELECON*, pp. 857 860, , Malaga, Spain, May 2006. DOI: 10.1109/MELCON.2006.1653233.

[47] K. Srinivasan, C. Lafond, R. Jutras, "Short-Circuit Current Estimation from Measurements of Voltage and Current During Disturbances", *IEEE Transactions on Industrial Applications*, vol. 33, no.4, Jul. 1997. DOI: 10.1109/28.605749.

[48] ACTOM, "Distribution Transformers Brochure". [Online]. Available from: www.actom.co.za

[49] Distribution Transformers – Edition 4, SANS 780:2009, 2009.

[50] J. Marks, O. Krause, D. Martin, D. McPhail, "Using Power State Estimation to Calculate Hotspot Temperature of Distribution Transformers", in *Proceedings of IEEE PES Asia-Pacific and Energy Engineering Conference*, pp. 1- 5, 2015. DOI: 10.1109/APPEEC.2015.7381070.

[51] M. Khanali, S. Jayaram, J. Cheng, "Effects of Voltages with High-Frequency Contents on the Transformer Insulation Properties", in *Proceedings of Electrical Insulation Conference*, pp. 235 – 238, Canada, Jun. 2013. DOI: 10.1109/EIC.2013.6554240

[52] N. Jayasighe, J. Lucas, K. Perera, "Power System Harmonic Effects on Distribution Transformers and New Design Considerations for K Factor Transformers", presented at *IEEE Sri Lanka Annual Sessions*, Sep. 2003.

[53] D. Said, K. Nor, M. Majid, "Analysis of Distribution Transformer Losses and Life Expectancy using Measured Harmonic Data", in *Proceedings of 14th International Conference on Harmonics and Quality of Power*, pp. 1 – 6, 2010. DOI: 10.1109/ICHQP.2010.5625404

[54] G. Chicco, F. Corona, R. Porumb, F. Spertino, "Experimental Indicators of Current Unbalance in Building-Integrated Photovoltaic Systems", *IEEE Journal of Photovoltaics*, vol. 4, no. 3, May 2014. DOI: 10.1109/JPHOTOV.2014.2307491

[55] D. Gallo, R. Langella, A. Testa, "Case Studies on Large PV Plants: Harmonic Distortion, Unbalance and their effects", presented at *IEEE Power & Energy Society General Meeting*, pp. 1 – 5, 2013. DOI: 10.1109/PESMG.2013.6672271

[56] S. Heunis, M. Dekenah, "A load profile prediction model for residential consumers", *Energize Magazine*, pp 46 – 49, May 2010.

[57] R. Kordkheili, B. Bak-Jansen, J. Pillai, B. Bhattarai, "Improving and handling electric vehicle penetration level by different smart charging algorithms in distribution grids", presented at *IEEE Eindhoven PowerTech*, pp. 1 – 6, Netherland, 2015. DOI: 10.1109/PTC.2015.7232571

ADDENDUM A CONSUMPTION SURVEY

Electricity consumption survey		Complex name	
Unit no.		Date of interview	
Number of occupants		Time of interview	
Occupation			
Working hours			

Appliance	Power rating	Start Time 1 (Duration)	Start Time 2 (Duration)	Start Time 3 (Duration)
Geyser	(2600 W)			
Stove	(3000 W)			
Kettle	(2000 W)			
Fridge	(160 W)			
Other (hair dryer, Iron)	(1200 W)			
Electronics	(100 W)			
Heating / Air conditioning	(1200 W)			

Monthly energy usage		kWh	

ADDENDUM B POWER QUALITY STANDARDS

Addendum B contains a summary of power quality standards applicable to high density residential complexes containing embedded generation. The South African power quality standards are mostly derived from the IEC and IEEE standards.

1. **Grid Connection Code for Renewable Power Plants (RPPs) connected to the Electricity Transmission System (TS) or the Distribution system (DS) in South Africa**

According to the grid connection code, the PV systems contemplated in this research fall into category A1 which comprise of RPPs rated less than 13.8 kVA.

- The PV generators rated larger than 4.6kVA must be 3-phase connected.
- The PV generators are required to operate continuously under voltage variations from -15% to +10%.
- The PV generators must survive a rate of change of frequency of 1.5Hz/s
- The PV generators must survive phase jumps of 20° and operate continuously.
- The PV generators must survive voltage dips to 0.6pu for 150ms
- The PV generators must survive voltage dips to 0.8pu for 600ms
- The PV generators must trip in less than 200ms after the voltage falls below 0.5pu
- The PV generators must operate at unity power factor

2. **NRS 048 Quality of Supply**

- Unbalance planning level of low voltage networks is 1.5%

3. NRS 097-2-3:2014 Grid Interconnection of Embedded Generation – Small Scale embedded generation

- The total generation connected to a shared feeder should not exceed 25% of the MV/LV transformer rating.
- Penetration level of 30% to 50% of individual customers connecting to a shared feeder.
- Where there are copper cables longer than 500m or aluminium cables longer than 350m, the maximum generation capacity may be further reduced or larger current cables may be required.
- The total MV feeder generation should be less than 15% of the peak load.
- Voltage variation at the customer supply point should be between 10%
- Maximum change in LV voltage due to embedded generators < 3%
- Islanding of the distribution grid is not allowed
- Apportioned voltage unbalance permitted is 0.5%

The maximum harmonic currents allowed to be injected by a device in an LV grid are given in Table B.1.

Table B.1 NRS097 2-3 Harmonic current limits

Odd harmonic		Even Harmonic		Inter harmonic	
#	[%]	#	[%]	#	[%]
3	3.00	2	0.75	1.5	1.00
5	1.50	4	0.38	2.5	0.60
7	1.00	6	0.25	3.5	0.43
9	0.70	8	0.19	4.5	0.33
11	0.50	10	0.15	5.5	0.27
13	0.40	12	0.13	6.5	0.23
15	0.25	14	0.11	7.5	0.20
17	0.30	16	0.09	8.5	0.18
19	0.25	18	0.08	9.5	0.16
21	0.18	20	0.08	10.5	0.14
23	0.20	22	0.07	11.5	0.13
25	0.15	24	0.06	12.5	0.12
27	0.14	26	0.06	13.5	0.11
29	0.13	28	0.05	14.5	0.10
31	0.12	30	0.05	15.5	0.10

Table B.2: NRS 048 Part 4 Harmonic voltage limits

Harmonic	Planning	Compatibility		Harmonic	Planning	Compatibility
#	%	%		#	%	%
				2	1.50	2.00
3	2.00	5.00		4	1.00	1.00
5	2.00	6.00		6	0.50	0.50
7	2.00	5.00		8	0.40	0.50
9	1.00	1.50		10	0.40	0.50
11	1.50	3.50		12	0.20	0.46
13	1.50	3.00		14	0.20	0.43
15	0.30	0.50		16	0.20	0.41
17	1.00	2.00		18	0.20	0.39
19	1.00	1.76		20	0.20	0.38
21	0.20	0.30		22	0.20	0.36
23	0.70	1.41		24	0.20	0.35
25	0.70	1.27		26	0.20	0.35
27	0.20	0.20		28	0.20	0.34
29	0.63	1.06		30	0.20	0.33
31	0.60	0.97		32	0.20	0.33
33	0.20	0.20		34	0.20	0.32
35	0.56	0.83		36	0.20	0.32
37	0.54	0.77		38	0.20	0.32
39	0.20	0.20		40	0.20	0.31

ADDENDUM C LOAD HARMONIC EMISSIONS

Table C.1: Typical electronic load harmonic current emission

	CFL		TV/PC Monitor		PC	
Harm #	% Fund	mA	% Fund	mA	% Fund	mA
1	100	250	100	650	100	800
3	90	225	98	637	97	776
5	75	187.5	91	591.5	91	728
7	56	140	83	539.5	82	656
9	39	97.5	73	474.5	73	584
11	28	70	62	403	63	504
13	22	55	50	325	51	408
15	22	55	39	253.5	40	320
17	22	55	28	182	30	240
19	20	50	18	117	22	176
21	18	45	11	71.5	15	120
23	17	42.5	8	52	10	80
25	17	42.5	8	52	5	40
27	16	40	9	58.5	2	16
29	15	37.5	9	58.5	2	16
31	14	35	8	52	1	8